Electronic Research Archive

ERA, 33(4): 1902–1945.
DOI: 10.3934/era.2025086
Received: 04 February 2025
Revised: 27 March 2025
Accepted: 31 March 2025
Published: 03 April 2025

http://www.aimspress.com/journal/ERA

Research article

Robustness analysis of a multimodal comprehensive transportation network from the perspectives of infrastructure and operation: A case study

Jialiang Xiao[1,2,3], Yongtao Zheng[1,2,3], Wei Wang[1,2,3,*] and Xuedong Hua[1,2,3]

[1] Jiangsu Key Laboratory of Urban ITS, Southeast University, Nanjing 211189, China
[2] Jiangsu Province Collaborative Innovation Center of Modern Urban Traffic Technologies, Nanjing 211189, China
[3] School of Transportation, Southeast University, Nanjing 211189, China

* **Correspondence:** Email: wangwei_transtar@163.com; Tel: +8618805151959.

Abstract: The development of a multimodal comprehensive transportation network (CTN) is crucial for enhancing connectivity and resilience in a regional transportation system. While China has established an extensive transportation infrastructure, the robustness of multimodal transportation systems remains insufficiently explored. Existing research primarily examines transportation networks from a single aspect, focusing either on infrastructure attributes or operational characteristics, while largely neglecting their interactions and disparities. To address this gap, this study analyzed the robustness of CTN from two perspectives, including a comprehensive transportation infrastructure network (CINet) and comprehensive transportation operation network (CONet). Based on complex network theory, optimized modeling methods of the networks were proposed. Utilizing multi-source data, statistical characteristics and robustness were comparatively explored in CINet, CONet, and their single-mode networks including highway, railway, navigation, and airway/airline (HINet, RINet, NINet, AINet, HONet, RONet, NONet, AONet) networks of Jiangsu Province. The results reveal that: 1) In Jiangsu, all the networks are not scale-free. All infrastructure networks (INets), except for AINet, do not exhibit small-world properties, while all the operation networks (ONets) are small-world. 2) All the networks are more robust to random attack than other strategies. CINet demonstrates the highest robustness among INets, whereas surprisingly, RONet is the most robust among ONets. Generally, INets exhibit superior robustness compared to ONets. 3) As the number of optimized hubs increases, the network robustness is much stronger, especially under calculated attacks. The improvements of IRC and IRR reach 4.55% and 114.56% in CINet, while reaching 4.10% and 99.24% in CONet, respectively, indicating a significant effect of optimized hub designs in network robustness

enhancement. 4) When optimizing the same hubs, network robustness enhancement is more pronounced in CONet than in CINet. These findings highlight the importance of optimized hubs to multimodal comprehensive transportation systems, and provide guidance for network planning and management.

Keywords: comprehensive transportation infrastructure network; comprehensive transportation operation network; network modeling method; network robustness analysis

1. Introduction

Comprehensive transportation networks (CTNs) can be divided into two perspectives: a comprehensive transportation infrastructure network (CINet) and comprehensive transportation operation network (CONet). They can mutually influence each other in that the CINet serves as the foundation for the CONet, while the CONet provides guidance for the planning and maintaining of the CINet [1,2]. In order to improve the commuting efficiency of CTNs and promote economic development, the CINet and CONet ought to be robust. Previous studies have primarily focused on the robustness of different modes of transportation networks within a city or regional area, such as highway networks [3], railway networks [4,5], and public transit networks [6], typically from a single perspective. However, there remains a gap in the construction and joint analysis of a multimodal CINet and CONet within the same CTN, thereby hindering a comprehensive understanding of their interplay and differences in network statistical characteristics and robustness.

Furthermore, traditional multimodal CTNs only represent a hub with a single vertex [7], disregarding the internal transfers and external connections of the hub. This may underestimate the bridging role and importance of the hub in CTNs and can lead to a greater negative effect on network robustness when hub vertex failure occurs. Therefore, optimized designs of the hub must be considered when modeling the CINet and CONet, respectively. Based on the aforementioned issues, three questions urgently need to be addressed. The first is what the differences in robustness between the CINet and CONet are. The second is what characteristics the CINet and CONet exhibit when considering the optimized transfer design of the hub. The third is how much the optimized hub can enhance network robustness.

Based on the above research objectives, Jiangsu Province, a typical economically developed province in China, is selected for a case study. The CTN of this area is a multimodal network that includes highways, railways, navigations, and airways/airlines. The network also exhibits well-established infrastructure and encompasses a large number of operational lines. Accordingly, the analysis of multimodal infrastructure networks and operation networks in Jiangsu can reflect their statistical and robustness characteristics and provide valuable insights for network planning, construction, and management throughout China.

This paper has four contributions: 1) The statistical and robustness characteristics of the infrastructure networks and operation networks are analyzed comparatively. Several indicators are employed to conduct robustness comparative analysis of different modes of infrastructure networks and operation networks under four attack strategies. 2) Optimized modeling methods for the hub in the CINet and CONet are proposed, respectively, and a before-and-after comparative analysis is conducted to evaluate the effect of the hub optimization on network robustness. We analyze how much the

robustness of the CINet and CONet can be improved with the application of the optimized hubs. Furthermore, we demonstrate the robustness improvement as the number of optimized hubs increases, which examines the validity of our proposed modeling methods. 3) The impact of the failure of the same scale hubs on network robustness is explored. We comparatively analyze how much the robustness of the CONet is affected by the failure of the hubs of the same scale in the CINet but varying degrees in the CONet. 4) Various suggestions are provided from multiple perspectives to enhance the planning of the hubs, the construction of hub channels, and the management of the operational lines in the CINet and CONet, aiming to contribute to the improvement of transportation environments.

The research contents are as follows: Section 2 reviews the literature and identifies the previous research gaps for further improvement. Section 3 proposes optimized modeling methods for the CINet and CONet, respectively. Section 4 describes the case and introduces analytical methods and indicators of network robustness. Section 5 conducts comparative analyses for the robustness of different modes of infrastructure networks and operation networks. Section 6 discusses the improvement of hub optimization on the robustness of the CINet and CONet with various experiments. Section 7 summarizes the conclusions and provides some suggestions.

2. Literature review

2.1. Research of the transportation network

The transportation network serves as an abstract representation of the transportation system, encompassing various critical elements such as transportation infrastructure, transportation routes and, traffic demands. Previous research on transportation networks has primarily focused on different modes of transportation infrastructure networks or operation networks within cities or regional areas. For the infrastructure networks (INets) [8,9], the elements are supposed to center on some realistic transportation infrastructure entities. The nodes in the INet usually include airports, railway stations, intersections, wharves, and toll stations, which can reflect their basic transportation functions and locations in the real world. The edges in the INet represent realistic sections, which incorporate attributes such as section length, section levels, section types, and speed limits. Zhang [10] developed a multi-scale robustness model for a real-world highway network, considering the occurrence of flood hazards. Zhu [11] constructed the arterial highway networks of Xinjiang and employed four attack strategies on the network for robustness assessment based on multi-hazard information. Vani [12] focused on the large-scale transportation road network in the province of Ontario, Canada, modeled the truck and passenger flows of the network, and utilized network-wide travel time to evaluate the network robustness when encountering the closure of each link in the network.

However, the operation networks (ONets) focus on the information of different modes of operational lines. Consequently, compared to the infrastructure networks, the edges in the ONet represent the virtual operational routes or schedules, rather than realistic sections [13]. Yang [14] established the rail transit network according to 18 operational subway lines in Beijing and developed a weighted composite index for node importance assessment. Ma [15] constructed the bus-subway double-layered network based on public transit stations and lines in the Xicheng District of Beijing. The network robustness was systematically evaluated under intentional attacks with structural and functional indicators. Aiming to measure the node importance, Wandelt [16] imposed seven airports and 16 flights to construct the air transport network and proposed an integer program formulation for airline recovery when facing node disruptions.

Apparently, although existing studies have devoted efforts to analyzing the transportation networks from different perspectives, distinctions between the INets and ONets within the same transportation system remain insufficiently explored.

2.2. Construction of the multimodal transportation network

Transportation networks can be divided into single-mode networks and multimodal networks. Extensive efforts have been devoted to the study of single-mode networks, such as urban transit networks [17,18], railway networks [19,20], and aviation networks [21]. Zanin [22] analyzed the global aviation network structure variation for the period from 2011 to 2022, and identified the node importance to reveal the critical nodes in the system. Sugishita [23] investigated the delay propagation patterns of Japan's domestic air transport network and explored the spreading delays characteristic by comparing the delay causality networks with corresponding randomized networks.

Compared to single-mode transportation networks, multimodal networks are mainly constructed as a multilayer network with different single-mode networks. Therefore, it requires increased attention to the transitions and connections between different layers. Two basic methods are commonly used for constructing multimodal transportation networks:

1) Supernetwork model

The supernetwork is a complex network model that integrates different sub-networks into a composite multilayer network. Each layer of the sub-network can connect with others by virtual segments, thus generating a mutually nested and interconnected multilayer network [24,25]. Many scholars have applied this method to the construction of urban transportation networks and regional transportation networks. Michel [26] employed the supernetwork model to establish a multimodal transportation network including highways, railways and waterways, and analyzed the traffic assignment problem of freight demands in the network. Xu [27] constructed a multimodal supernetwork for urban agglomerations and introduced a stochastic equilibrium assignment model for intercity transportation systems. Ding [28] modeled the entire process of passengers' urban public transit travel with the supernetwork, and conducted the transit network assignment considering the transfers of different bus lines.

2) Merging model

The merging model achieves the integration of different modes by combining the nodes and routes from multiple sub-networks in order to construct a multilayer network. For example, in the construction of urban bus-subway composite networks [29], the adjacent bus stops and subway stations are merged into a single node to connect the bus network and the subway network. Based on two single-layer networks, Li [30] proposed the hub stations between the bus system and metro system as coupled nodes and added coupled edges for the coupled nodes to construct a composite bus-metro network. Feng [31] treated the railway stations and airports from different sub-networks as homogeneous nodes and considered the homogenous nodes in the same city as a single node. Buldyrev [32] merged the nodes of different modes within the same defined area into a hub node, which connected different sub-networks and established a multilayer complex network.

2.3. Transportation network robustness analysis

Research on transportation network robustness analysis has mainly focused on various kinds of single-mode transportation networks, including urban transit networks, subway networks, railway networks, and aviation networks. Berche [33] analyzed the robustness of the public transport networks

of 14 major cities in the world by different attack strategies and derived vulnerability criteria for exploring the minimal strategy with the highest negative effect on the public transport network. Chen [34] utilized complex network theory to analyze the robustness of multimodal urban transport networks in Beijing with topological indicators, and the Monte Carlo method was applied to simulate the random attacks to the network. Ge [35] established an urban public transport network and explored the relationship between different disturbances and network robustness. Hu [36] employed the space-L method to generate the high-speed railway network in China and evaluated its network robustness with indicators from the perspectives of network topology and functionality. Yang [37] considered the temporal attributes and dynamic connections of the Chinese aviation temporal network based on the flight schedules and operation information. Moreover, with the improvement of artificial intelligence models, some studies have applied them to robustness analysis and the optimization design of transportation networks [38–40]. Liu [41] proposed an improved language model for transportation network design optimization and robustness enhancement to solve the delivery route problem.

According to studies on the robustness of different transportation networks, it can be observed that most networks exhibit weaker robustness under calculated attacks, whereas they can withstand more attacks and experience delayed network failure under random attacks [34,42]. Ma [43] analyzed the robustness of the Nanjing urban rail transit network by considering various load distribution methods and different attack strategies. It revealed that the intentional attack strategy was more destructive to the transport capacity than the random attack strategy, and the robustness under static intentional attack was weaker than that under dynamic intentional attack. Li [44] conducted a vulnerability analysis on a public transport network and found that simultaneous calculated attacks to different components in the network significantly impacted the network robustness. Chen [45] explored the robustness of China's air transportation network (CATN) over 40 years under different attack strategies. CATN exhibited enhanced robustness under random attacks where the network paralysis only occurred when over 80% of the airports were destroyed. However, under targeted attacks, only 20% of the airport failures could destroy CATN.

According to the previous studies, the indicators for robustness evaluation can be divided into network topology-based indices and transportation operation indices. The former indicators include centrality [46], clustering coefficient [47], maximum connectivity graph [48], and global efficiency [49], which quantify the degree of damage to the network structure under a certain attack. On the contrary, the latter analyzes transportation robustness from the operational perspective, which considers the impact of the disruptions on the traffic demands or transportation operations. Travel time, passenger flow, and capacity degradation are commonly used indicators in such works [50,51]. Jiang [52] introduced the remaining carrying capacity to measure the robustness of a bilayer railway-aviation transportation network, and explored the interaction effects of various modes when encountering multiple attack scenarios. Zhang [53] proposed a vote rank algorithm to identify the critical stations of the urban rail transit network and analyzed its structural and functional robustness by global efficiency, largest connected subgraph, and passenger travel cost.

In addition, some scholars have combined topology-based indices and operation indices to systematically analyze the robustness of transportation networks. Zhang [54] combined the static metrics such as betweenness and closeness with the dynamic metrics like flow degree to analyze the robustness of the urban railway network cascading failures in Hong Kong. Liu [55] proposed a comprehensive assessment index considering network function, structure, and recovery performance to explore the resilience of the urban road networks under different attack scenarios.

2.4. Summary of the literature

Although researchers have made significant progress in studying transportation network robustness, several gaps still exist and require further exploration and optimization.

Lack of analysis on the differences and unique characteristics of various perspectives of networks within the CTN: Previous research mainly investigates the transportation network from a single perspective, focusing either on the INets or ONets. However, limited research has been conducted on a joint analysis of the CINet and CONet. Accordingly, several questions remain unexplored. Q1: What are the similarities and distinctions of the modeling objectives between the CINet and CONet? Q2: What are the mapping rules for constructing the network topology of the CINet and CONet? Q3: How do the robustness and statistical characteristics perform in the CINet and CONet, respectively? These questions will be addressed in Sections 3.1 and 5.1–5.3.

Lack of detailed design for modeling the multimodal transportation network: Previous studies primarily concentrate on the modeling of single-mode or composite networks, such as bus-subway transit networks, railway networks, and aviation networks. For the construction of multimodal transportation networks, supernetwork and merging models are two commonly utilized methods. However, these two models neglect the detailed design of the transfers and connections between different transportation modes, which leads to deviations from real-world transportation systems. Two critical questions remain to be addressed. Q4: How to conduct the detailed design in the CINet and CONet, respectively, when modeling the multimodal transportation network? Q5: How does the detailed design influence the robustness of the CINet and CONet? The two questions will be answered in Sections 3.2 and 3.3 and Sections 6.1 and 6.2.

Insufficient comparative analysis of the network robustness in a multimodal transportation network: Previous studies have only explored the trends of the robustness performance of multimodal transportation networks under external disturbance. However, several research gaps exist when analyzing the network robustness. Q6: Are there any differences in robustness between single-mode and multimodal transportation networks? Q7: What are the disparities in robustness between the CINet and CONet? Q8: How does the failure of the same hub vertex affect the robustness of the CINet and CONet? These questions will be addressed in Sections 5.2–5.4.

3. Network modeling method

3.1. Network structure of the CINet and CONet

The CTN is an abstract representation of the comprehensive transportation system which includes traffic facilities, traffic lines, and other elements of multiple transportation modes in a regional area. Besides, the CTN can be divided into two aspects: the CINet, which reflects the real traffic entities, and the CONet, which expresses the operation information of several traffic entities.

The CINet is a complex system with multiple modes that combines all the public infrastructure facilities of highway, railway, navigation channel, and airway networks, where its elements include airports, wharfs, intersections, etc. It comprises four kinds of single-mode infrastructure networks and the micro-network of transit hubs. Single-mode infrastructure networks refer to highway, railway, navigation, and airway transportation networks (HINet, RINet, NINet, and AINet, respectively). The micro-network of transit hubs includes the transfer network inside the hub and the connecting sections outside the hub. The transit hub point (THP) is defined as the vertex with a mode transfer function, which includes the vertices of railway stations, harbors, and airports.

The CONet is a complex network which primarily describes the operational information of a transportation system, including the basic physical topology structure of the network, different modes of operational lines, etc. Apparently, the physical structure of the CONet is constructed based on real-world transportation facilities. The nodes in the CONet refer to the entities with transportation operation functions, such as railway stations and airports, while the edges depict the operational information between any two nodes. For example, if there is a direct operational line between vertex A and vertex B in the CONet, an edge is established between them.

Therefore, without the transportation infrastructure facilities in the CINet, it would be impossible to map the operational information and build the operation network. Furthermore, the CONet comprises four types of single-mode operation networks, the mode transfer network inside operation hubs, and the connection network of intra-city operation vertices. Single-mode operation networks refer to highway, railway, navigation, and airline operation networks (HONet, RONet, NONet, AONet, respectively). The mode transfer network inside operation hubs represents the mode transfer activities of passengers inside the hub, while the connection network of intra-city operation vertices can reflect the phenomenon that people transfer among different stations within a city. Moreover, the operation hub point (OHP) is defined as the operation vertex that connects multiple transportation modes of operational lines.

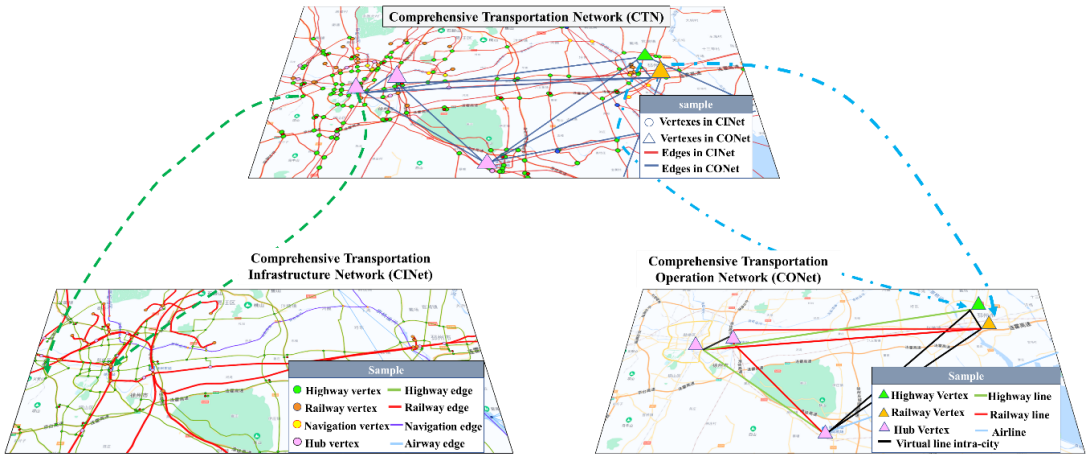

Figure 1. The structure of the CTN.

The CINet can be described as $G_{CI} = (V_{CI}, E_{CI})$, where V_{CI} and E_{CI} refer to the set of vertices and edges in the CINet. Similarly, HINet, RINet, NINet, and AINet can be denoted as $G_{HI} = (V_{HI}, E_{HI})$, $G_{RI} = (V_{RI}, E_{RI})$, $G_{NI} = (V_{NI}, E_{NI})$, and $G_{AI} = (V_{AI}, E_{AI})$, respectively. The set of the THP is defined as V_{THP}, and a THP is denoted by v_{THP}^k. The outside connecting section of v_{THP}^k is denoted as e_{P1P2}^k. The mathematical expression of the inside transfer network of THP is $G_T^k = (V_T^k, E_T^k)$, where V_T^k denotes the set of transfer vertices and E_T^k denotes the set of transfer edges.

The CONet is defined as $G_{CO} = (V_{CO}, E_{CO})$, while HONet, RONet, NONet, and AONet are similar. Besides, V_{CO} and E_{CO} refer to the set of vertices and edges in the CONet. The set of the OHP can be denoted as V_{OHP}, and the vertex of it is v_{OHP}^i. The mathematical expression of the mode transfer network inside the OHP is $G_O^i = (V_O^i, E_O^i)$, where V_O^i denotes the set of mode conversion vertices and E_O^i denotes the set of mode conversion edges.

The mapping rules of the elements in the CINet and CONet are clarified to abstract the network. The modeling objects and the meaning of the vertices and edges of different single-mode networks of the CINet and CONet are shown in Table 1.

Table 1. The establishment of mapping rules.

Mode	Modeling objects of the **infrastructure network**	Modeling objects of the **operation network**	Meaning of vertices and edges			
			V_{I^*}	V_{O^*}	E_{I^*}	E_{O^*}
Highway	National expressways, provincial expressways, national trunk highways, provincial trunk highways, urban expressways, and urban main roads	Long-distance bus operational lines (interprovincial, provincial, intercity, inter-county)	Plane intersection, stereo intersection, expressway entrances and exits, and toll stations	Bus stations (First class, Second class, Third class)	The main highway sections existing between two vertices	Long-distance bus operational lines
Railway	The national high-speed railway, the national heavy haul railway, and the national railway Grade I-III	The national high-speed railway lines and the national railway Grade I-III lines	The railway stations and the large overpasses intersected by two or more railway lines	Railway stations (Top-class, class I-III)	The main railway sections	Railway operational lines
Navigation	The navigation channel Grade I, II, III	Operational lines on navigable waterways	Wharves, locks in the inland waterway, and intersections of inland waterways	Harbors and ports (super-size, large size, medium-size, and small size)	Navigation channel sections	Navigation lines
Airway/ Airline	Airway	Airline	Airports, reporting points, VOR, DME, and NDB**	Airports (4F, 4E, 4D, and 4C class)	The airway sections	Airlines

*V_I and V_O refer to the vertices in the single-mode infrastructure network and operation network. E_I and E_O refer to the edges in the single-mode infrastructure network and operation network.

**VOR, DME, and NDB are the abbreviations of vertices with definite functions on the air route. VOR: Very High Frequency Omnidirectional Range. DEM: Distance Measuring Equipment. NDB: Nondirectional Beacon.

Differences in the mapping rules can be observed between the infrastructure and operation networks. It is obvious that the modeling objects of the infrastructure networks focus more on the real facilities and the existing roads, while the operation networks pay more attention to the operational information and operational lines among the existing public infrastructure facilities.

3.2. Modeling methods for the hubs in the CINet and CONet

3.2.1. Modeling method for the transit hub in the CINet

In a multimodal comprehensive transportation system, travelers often complete transfers between different transportation modes at hub nodes to facilitate long-distance travel. Therefore, designing the transfer channels at hub nodes is crucial for reflecting the realistic transportation network structure. The traditional composite network modeling methods in previous studies [24,25] generally overlook the transfer process and only utilize a single node to connect different modes of edges. Therefore, to abstractly represent the transfer behaviors and external connections of the real transportation network at a hub node, we propose a detailed modeling method for the transit hub in the CINet.

The transit hubs (THP) are applied to connect different single-mode transportation networks in the CINet, and the modeling method for a transit hub consists of the transfer network inside the THP and the connecting section outside the THP.

1) The transfer network inside the THP

To depict travelers' transfer process at the THP, the transfer network inside the THP is constructed to connect the transfer vertices of the hub in pairs by transfer edges. We define the transfer network of the transit hub v_{THP}^k as $G_T^k = (V_T^k, E_T^k)$. The number of the transfer vertices in v_{THP}^k depends on the number of the edges that connect to v_{THP}^k, regardless of their transportation modes. The transfer edges are generated according to the connections between any two transfer vertices. For example, v_{THP}^k is separated into four transfer vertices $v_1^k, v_2^k, v_3^k, v_4^k$ because there are four edges connected to v_{THP}^k originally. The transfer edges $e_{12}^k, e_{13}^k, e_{14}^k, e_{23}^k, e_{24}^k, e_{34}^k$ represent the connecting sections in v_{THP}^k.

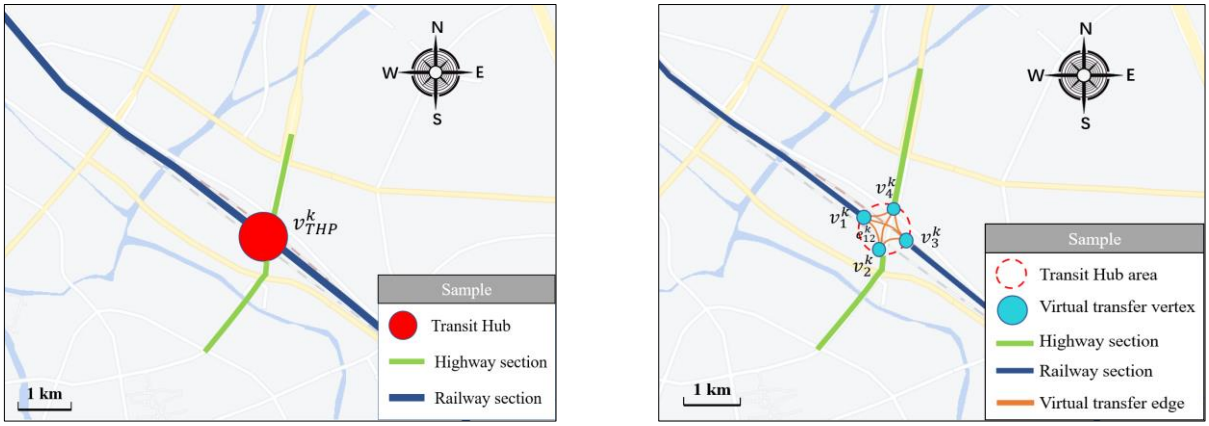

(a) (b)

Figure 2. Modeling of the transfer network inside the THP.

2) The connecting section outside the THP

According to Table 1, only high-grade highway sections are selected to construct the HINet. However, the transit hubs are often surrounded by slow traffic and connected to the low-grade roads. Hence, the transit hubs are unable to be connected to the HINet. The connecting section outside the THP is modeled to represent the low-grade highway section connecting the THP and the outside highway, as shown by the green edge in Figure 3. v_{THP}^k refers to the THP (a railway station), while v_{HI}^1 is a highway vertex, and e_{HI}^{1k} represents the connecting section outside the THP.

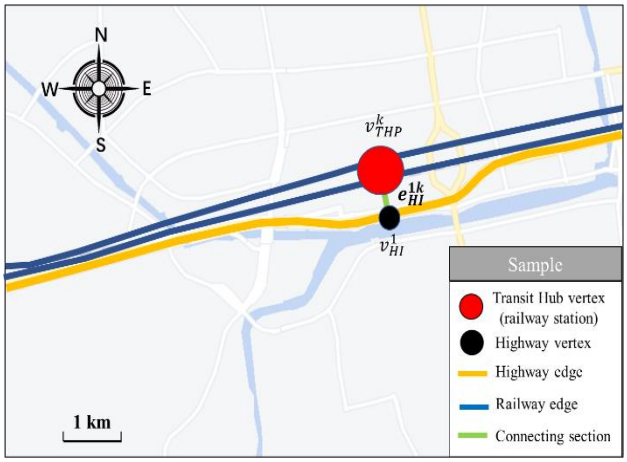

Figure 3. Modeling of the connecting section outside the THP.

3.2.2. Modeling method for the operation hub in the CONet

Compared with the THP in the CINet, the OHP only focuses on the conversion between different transportation modes, rather than the detailed transfer process from one road to another in the THP. Therefore, all operational lines of each transportation mode in the OHP are connected to a dedicated virtual transfer vertex. Subsequently, the virtual vertices of each mode are interconnected by virtual arcs, thereby depicting the mode conversion process within the OHP. As shown in Figure 4, the OHP v_{OHP}^{i} is separated into a highway virtual vertex v_1^i, a railway virtual vertex v_2^i, and an aviation virtual vertex v_3^i. The mode transfer edges represent the connecting sections between different single-mode transportation networks at v_{OHP}^{i}, such as e_{12}^{i}.

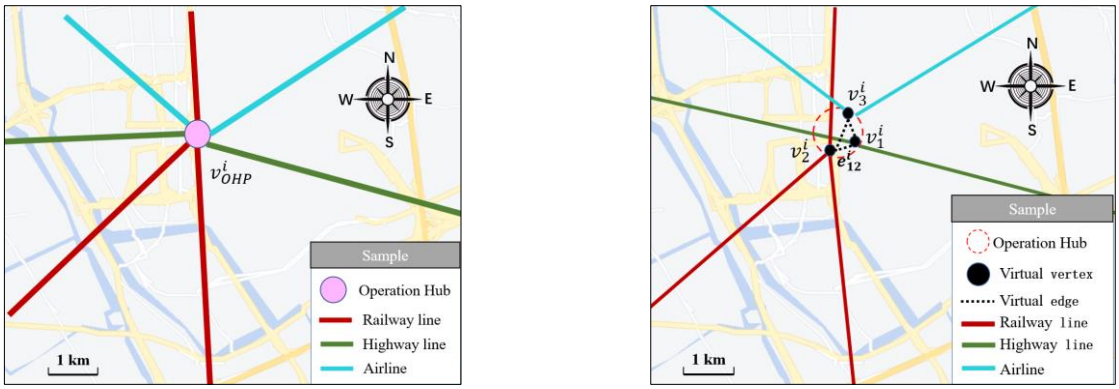

(a) (b)

Figure 4. Modeling of the mode transfer network inside the operation hub.

3.3. Modeling method for the connection network of intra-city operation vertices in the CONet

In reality, people often transfer between different stations within a city to complete a long-distance interregional trip, as shown in Figure 5. Passengers travel from Liyang railway station to Nanjing South railway station by high-speed train, then travel to Lukou airport by subway, and finally depart from

the airport to their final destination. Therefore, it is necessary to model the connection network of the intra-city operation network to abstract the above travel process. The modeling process can be divided into three steps.

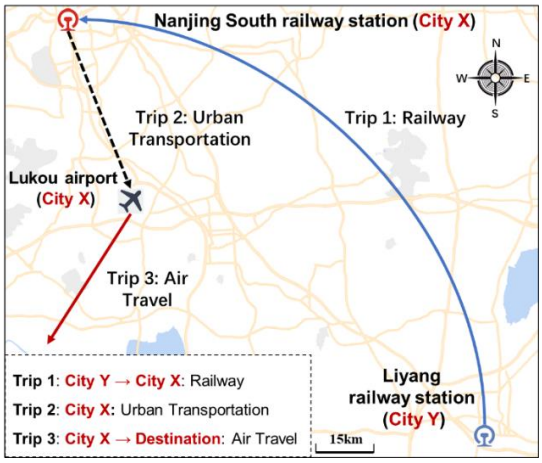

Figure 5. A long-distance interregional trip.

Step 1: Identifying the operation vertices within city X. According to the administrative division of different cities, the operation vertices belong to city X can be determined. Suppose that there are K operation vertices $\{v_{CO}^1, v_{CO}^2, \ldots, v_{CO}^K\}$ in city X, $CO = \{HO, RO, NO, AO\}$ in v_{CO}^i.

Step 2: Determining the service coverage of each operation vertices. The service coverage refers to a specific area, where travelers can travel directly from an operation vertex v_i to another intra-city operation vertex v_j within v_i's service coverage, without an additional transfer.

After acknowledging the operation vertices $\{v_{CO}^1, v_{CO}^2, \ldots, v_{CO}^K\}$ in city X, the service coverage area is determined based on the type and the class of each operation modeled.

Step 3: Generating the virtual edges between different operation vertices within city X.

The connecting rules of the virtual edges are as follows:

1) Each operation vertex $n_1 = v_{CO}^i$ only connects to the other vertices $n_2 = v_{CO}^j$ within its service coverage and generate a virtual edge $e_{city(X)}^{n_1,n_2}$.

2) If there exists a high-class vertex v_{CO}^i and a low-class vertex v_{CO}^j, whether they are connected only depends on the service coverage of the high-class vertex v_{CO}^i.

3) If there is an existing operation line $e_{CO}^{i,j}$ between v_{CO}^i and v_{CO}^i, then the virtual edge will not be generated.

All the virtual edges in city X can be generated according to the service coverage of each operation vertex and the above connecting rules. Figure 6 is an example for the connection network.

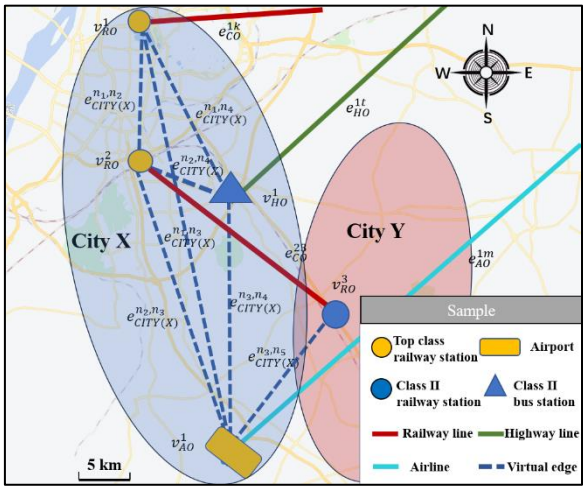

Figure 6. Modeling of the connection network of the intra-city operation vertices.

4. Case study and robustness analysis method

4.1. Data overview of the case

The case object is a CTN in Jiangsu Province, a typical coastal province in China. The highway, railway, and waterway data for constructing the CINet are derived from electronic navigation map data provided by NavInfo. The aviation data are derived from the Enroute Chart published by the Civil Aviation Administration of China (CAAC). The electronic navigation map data contains various information including transportation vertices, sections, points of interest (POIs), etc. Therefore, the data needs to be filtered according to the mapping rules in Section 3.1. After processing, the data spatial distribution is shown in Figure 7.

Corresponding to the CINet, the case object of the CONet is the operational lines of four transportation modes in Jiangsu Province as well. To obtain the operational information, the focused web crawler is applied to collect the ticket information or shipping information of highway intercity bus lines, railway lines, waterway lines, and airlines from Ctrip.com, 12306.com, shipxy.com, and variflight.com. A total of 22,277 pieces of valid data are acquired, and the sample is shown in Figure 8**.**

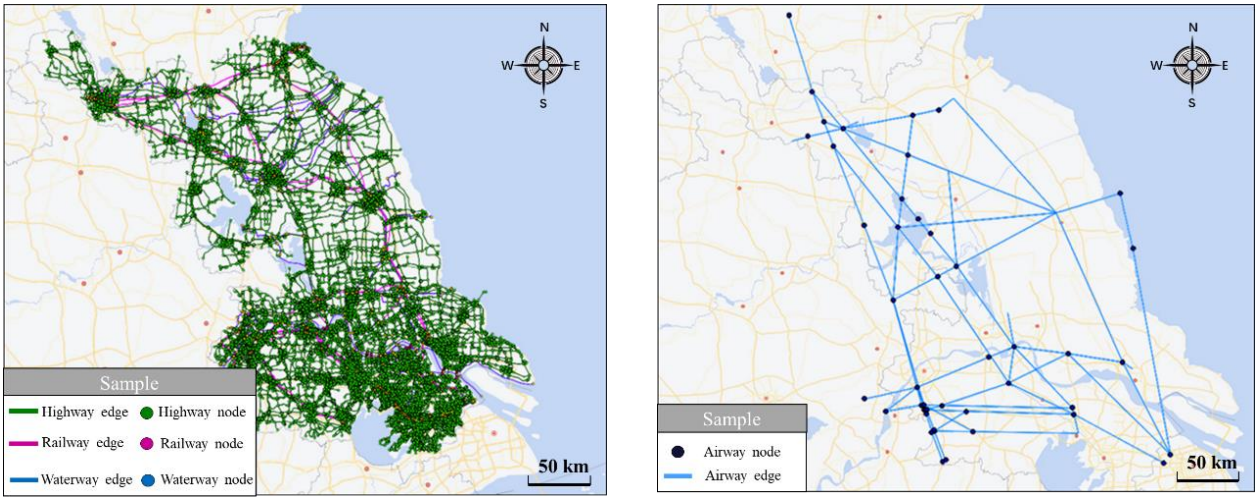

(a) Spatial distribution of the navigation map data (b) Spatial distribution of the CAAC enroute chart

Figure 7. Spatial distribution of infrastructure data for Jiangsu Province.

NO.	Lines	Origin	Destination	First class	Second class	Date of departure
1	G7035	Nanjing	Wuxi	YES	YES	20221005
2	D2281	Nanjing South	Wuxi	YES	YES	20221005
3	G7037	Nanjing South	Wuxi	YES	YES	20221005
4	G7001	Nanjing	Wuxi	YES	YES	20221005
5	G1509	Nanjing South	Wuxi East	7	YES	20221005
6	K781	Nanjing	Wuxi	8	9	20221004
7	G7043	Nanjing South	Wuxi	18	YES	20221005
8	G7039	Nanjing	Huishan	YES	YES	20221005
9	G7505	Nanjing South	Wuxi East	YES	NO	20221005
10	Z195	Nanjing	Wuxi	YES	YES	20221004
11	G7313	Nanjing South	Wuxi East	14	YES	20221005
12	G7271	Nanjing South	Wuxi	YES	YES	20221005

Figure 8. Sample data of operation information of the railway.

The crawled operational data includes various information such as the origin and destination of the line, the ticket price, seat class, etc. Therefore, it is necessary to process the data and construct the operation network. If there is at least one operation line between two operation vertices, an edge can be generated to connect them. Besides, the data is further filtered according to the operation network research objectives mentioned in Section 3.1. The data spatial distribution is shown in Figure 9.

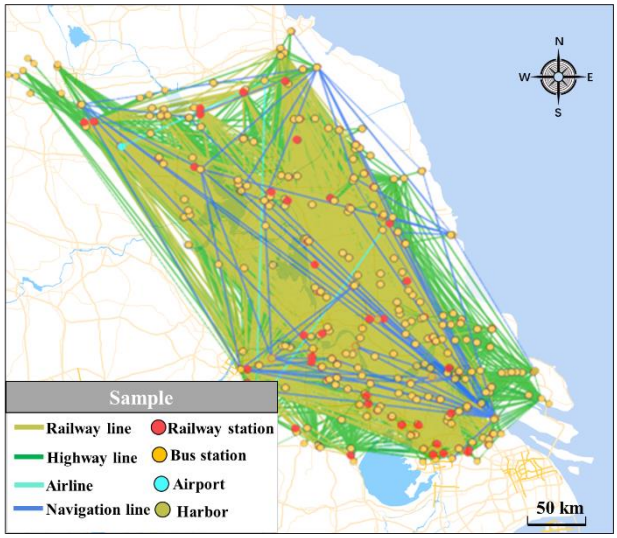

Figure 9. Spatial distribution of operation data for Jiangsu Province.

4.2. Robustness assessment index

4.2.1. Global efficiency $E(G)$ and its change $\eta(E(G)_T)$

Global efficiency $E(G)$ refers to the average of the reciprocal of the shortest path between two nodes in a network G, which can reflect the connectivity of the network. $E(G)$ is then calculated as follows:

$$E(G) = \frac{1}{N(N-1)} \sum_{i \neq j \in G} \frac{1}{d_{ij}} \tag{1}$$

where d_{ij} is the distance of the shortest path between vertex i and vertex j, and N refers to the number of vertices in network G. If there is no path between vertex i and vertex j, then $1/d_{ij} = 0$.

If a non-weighted network is completely connected, $E(G) = 1$. When the network is attacked and isolated vertices appear, the distance between vertices will continue to increase, and then $E(G)$ decreases.

Based on Eq (1), the change of global efficiency $\eta(E(G)_T)$ describes the network global efficiency when T vertices are attacked, and the equation of $\eta(E(G)_T)$ is as follows:

$$\eta(E(G)_T) = \frac{E(G)_T - \min\{E(G)_T\}}{\max\{E(G)_T\} - \min\{E(G)_T\}} \tag{2}$$

where $E(G)_T$ is the global efficiency of the network when T vertices are attacked, $T = 0,1,2,\ldots,N$. $\max\{E(G)_T\}$ and $\min\{E(G)_T\}$ represent the maximum and minimum values of $E(G)$ during the whole process of the attack. $\eta(E(G)_T)$ is a normalized index with $0 \leq \eta(E(G)_T) \leq 1$.

4.2.2. Change in maximal connected subgraph $\eta(R(G)_T)$

The maximal connected subgraph ratio $R(G)$ is used to measure the completeness of the network, that is, the ratio of the number of vertices in the maximal connected subgraph to the number of all vertices in the initial network. The equation of $R(G)$ can be defined as follows:

$$R(G) = \frac{MCG(G)_T}{N} \tag{3}$$

$$\eta(R(G)_T) = \frac{MCG(G)_T - \min\{MCG(G)_T\}}{N - \min\{MCG(G)_T\}} \tag{4}$$

where N is the number of all vertices in the initial network before attack. $MCG(G)_T$ is the number of vertices in the maximal connected subgraph of the network when T vertices are attacked, $T = 0,1,2,\dots,N$. $\eta(R(G)_T)$ is normalized with $0 \le \eta(R(G)_T) \le 1$. A higher $\eta(R(G)_T)$ indicates greater network robustness and better connectivity.

4.2.3. Standard structural entropy $H(G)$ and its change $\eta(H(G)_T)$

Structural entropy H is a critical metric used to quantify the uniformity of the network based on the degree distribution of vertices, where higher entropy indicates a more decentralized and less structured network. H is then calculated as follows:

$$H = -\sum_{i=1}^{N} I_i \ln I_i \tag{5}$$

$$I_i = \frac{k_i}{\sum_{i=1}^{N} k_i} \tag{6}$$

where H is the structural entropy of the network. I_i is the importance of vertex v_i and k_i is the degree of v_i.

To eliminate the influence of vertex numbers, standard structural entropy $H(G)$ is calculated as follows:

$$H_{\max} = \ln N \tag{7}$$

$$H_{\min} = \ln[4(N-1)]/2 \tag{8}$$

$$H(G) = \frac{H - H_{\min}}{H_{\max} - H_{\min}} = \frac{-2\sum_{i=1}^{N} I_i - \ln[4(N-1)]}{2\ln N - \ln[4(N-1)]} \tag{9}$$

where $H_{\max}$ is the maximum value of the structural entropy that all vertices have the same degree. $H_{\min}$ is the minimum value that all vertices directly connect to a special vertex.

The change of standard structural entropy $\eta(H(G)_T)$ describes the network standard structural entropy when T vertices are attacked (see Eq (10)).

$$\eta(H(G)_T) = \frac{H(G)_T - \min\{H(G)_T\}}{\max\{H(G)_T\} - \min\{H(G)_T\}} \tag{10}$$

where $H(G)_T$ is the standard structural entropy of the network when T vertices are attacked, $T = 0,1,2,\dots,N$. $\eta(H(G)_T)$ is a normalized index with $0 \le \eta(H(G)_T) \le 1$. The network is more robust and stable with a higher $\eta(H(G)_T)$.

4.2.4. Robustness composite index V

The robustness composite index V integrates the three aforementioned indicators, which is applied to evaluate the robustness of the network from multiple dimensions, including connectivity, completeness, and uniformity. The equation of V is as follows:

$$V = \lambda_1 \times \eta(E(G)_T) + \lambda_2 \times \eta(R(G)_T) + \lambda_3 \times \eta(H(G)_T) \tag{11}$$

where $\lambda_1, \lambda_2, \lambda_3$ refer to the weight of $\eta(E(G)_T)$, $\eta(R(G)_T)$, and $\eta(H(G)_T)$, respectively, which indicate the importance of connectivity, completeness, and uniformity to the network robustness. $\lambda_1, \lambda_2, \lambda_3 \in (0,1)$, and $\lambda_1 + \lambda_2 + \lambda_3 = 1.0 \leq V \leq 1$. The larger V is, the more robust the network. $\lambda_1 = \lambda_2 = \lambda_3 = 1/3$ is set in this research.

4.2.5. Critical ratio of network failure CR

The critical ratio of network failure CR describes the critical time point of network failure when the network is destroyed completely. The equation of CR is calculated as follows:

$$CR = \frac{CP}{N(G_0)} \times 100\% \tag{12}$$

$$CP = \varphi(V = 1\% \times V_0) \tag{13}$$

where CP refers to the critical point of network failure, which is the number of vertices that have been attacked when V is less than 1% of the value of the initial network V_0. CR is normalized with $0 \leq CR \leq 1$. The larger CR is, the more robust the network.

4.3. Experimental scheme for robustness analysis

Four attack strategies are proposed for robustness analysis, including random attack (RA), calculated attack (CAR), calculated attack considering update degree (CAUD), and calculated attack considering random selection (CARS). One vertex is attacked (removed from the network) at each round, and the corresponding edges of it are also deleted.

Among the four strategies, RA randomly attacks one vertex at a time without considering the difference between the vertices. CAR refers to a deliberate attack based on the vertex's degree. The vertex with a higher degree is more likely to be attacked earlier. However, some vertices have the same degree during the attack process. To clarify the attack sequence of these vertices, CAUD and CARS are employed for vertex attacks. CAUD updates the degree of the remaining vertices after each round of attacks and subsequently selects the one with the highest degree for the next attack. CARS randomly selects one vertex from the remaining vertices with the highest degree, and the selected vertex will be attacked in the next round. The steps of the four attack strategies are shown in Figure 10.

Based on these four strategies, we conduct attacks on the infrastructure networks and the operation networks separately. Then, the robustness characteristics of different networks are investigated by the aforementioned robustness assessment indicators.

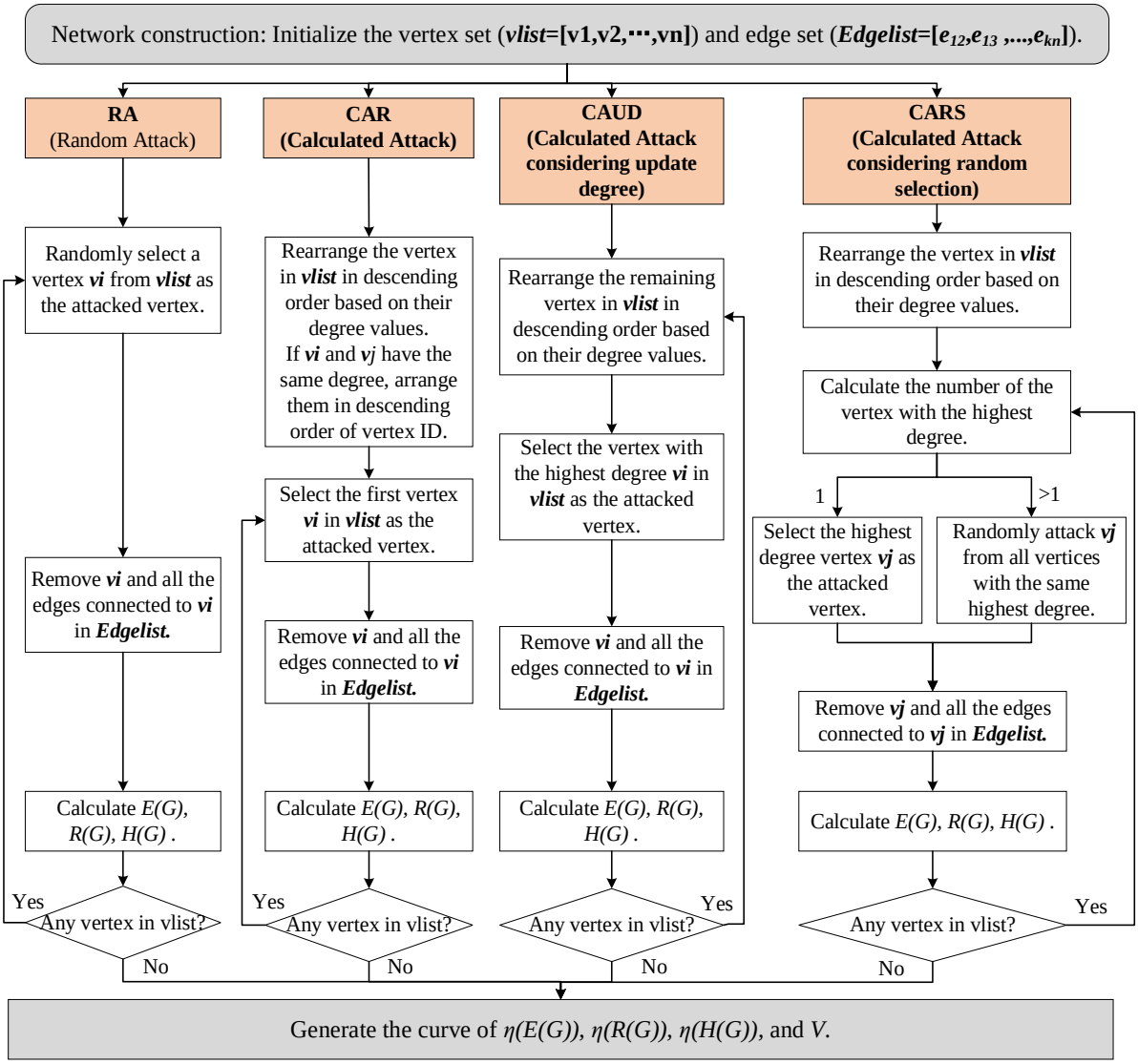

Figure 10. Steps of the four attack strategies on a network.

5. Network robustness analysis results

5.1. Statistical analysis for infrastructure networks and operation networks

5.1.1. Degree distribution

Figure 11(a) illustrates the degree distribution of five infrastructure networks. It is evident that the degrees of these networks are predominantly concentrated within the range of 1 to 4, with a limited number of high-degree vertices. Specifically, the degree distributions of the HINet and CINet are relatively similar in that their degrees are concentrated between 2 to 4 (accounting for 94.4% and 88.7% of the vertices, respectively). This indicates that highway transportation is the dominant transportation mode in a multimodal comprehensive transportation system, and the HINet serves as the backbone of the CINet. In contrast, the degrees of the RINet and AINet are concentrated between 1 to 3 (86.3% and 69.0%, respectively). However, the AINet features a higher proportion of high-degree vertices (15.5%), whereas the RINet has a lower proportion (2.0%). The degree distribution of the NINet is relatively

narrow, spanning from 1 to 4, mainly concentrated between 2 to 3 (79.1%). It can also be observed that approximately 99.76% of the vertex degrees in the HINet are less than 4, indicating that the intersection structures in the HINet mainly consist of four-way and three-way junctions, while only a few intersections involve more than four roads.

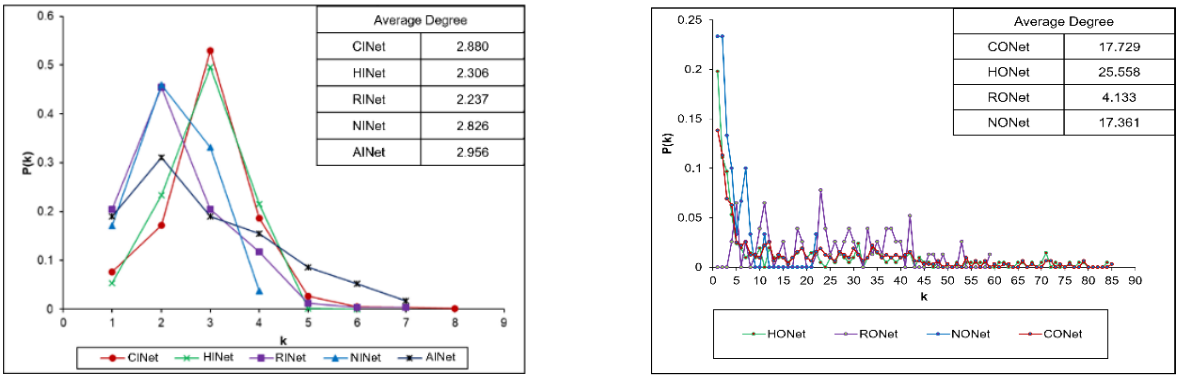

(a) Infrastructure network (b) Operation network

Figure 11. Distribution of different mode infrastructure networks and operation networks.

Given that the number of direct airlines among different airports in Jiangsu Province is small (only 3 airlines), the AONet, although not constructed individually, is taken into consideration within the CONet. Figure 11(b) illustrates the degree distribution of four operation networks. Compared with the results of the infrastructure networks, the average degrees of the operation networks are generally larger and there are more high-degree vertices (up to 90 in the CONet, and 84 in the HONet respectively). However, the proportion of vertices for each high degree value is relatively small, reflecting that there are fewer high-degree hubs in a network. Additionally, the low degree vertices of the CONet, HONet, and NONet are relatively concentrated. 54.8% of the vertices in the CONet have a degree less than 9 ($p(k \leq 9)_{CO}$ =54.8%), and 52.2% of the vertices in the HONet have a degree less than 6 ($p(k \leq 6)_{CO}$ =52.2%), while 60.0% of the vertices have a degree less than 3 in the NONet ($p(k \leq 3)_{CO}$ =60.0%). In contrast, the RONet exhibits a more dispersed distribution, where the proportion of vertices with different degrees is approximately equal. Only 25.9% of the vertices have a degree less than 12 in the RONet.

Compared to the infrastructure networks, the operation networks exhibit a relatively higher average degree and a more dispersed degree distribution. This is because the operation networks primarily reflect operational information between different vertices, where an edge can be established as long as an operational line exists between two vertices. However, the infrastructure networks mainly reflect the relative positions and topological relationships of physical transportation entities. As a result, the infrastructure networks have fewer connections, leading to lower degrees and a more concentrated degree distribution.

5.1.2. Scale-free and small-world properties

The degree distribution curve of the network is fitted using a power-law distribution function under a double logarithmic coordinate system to identify the scale-free property of the network. If the function's slope is $2 < \gamma < 3$, the network is considered as a scale-free network. When $\gamma > 3$, the network has the characteristics of both a random and scale-free network. As shown in Table 2, most of the networks are not scale-free, but only the AINet has a scale-free property.

Additionally, two indicators are calculated to explore the small-world property. When $\langle d\rangle \approx \frac{\ln N}{\ln\langle k\rangle}$, the network is small-world. As shown in Table 2, among the five infrastructure networks, only the AINet exhibits the small-world property, while the other four do not. It also turns out that all the operation networks have a small-world property, revealing the fact that the connection between any two points in operation networks is more direct and the operational lines of different modes are well designed based on developed infrastructure facilities in Jiangsu Province.

Table 2. Indicators of the network statistics properties**.**

Property	Indicator	Infrastructure Network					Operation Network			
		HINet	RINet	NINet	AINet	CINet	HONet	RONet	NONet	CONet
Scale-free	Power-law γ	-5.87	-4.29	-3.42	-2.07	-3.98	-0.662	-0.278	-0.828	-0.99
	$\frac{\ln N}{\ln k}$	7.649	6.632	3.586	3.586	7.710	1.85	1.34	2.39	2.085
Small-world	$\langle d\rangle$	26.98	12.478	4.205	4.205	22.58	2.449	1.715	2.161	2.881
	Small-world?	NO	NO	NO	YES	NO	YES	YES	YES	YES

5.2. Robustness analysis for the infrastructure networks

5.2.1. Robustness analysis for single-mode infrastructure networks

The four single-mode infrastructure networks exhibit various levels of robustness under different attack strategies. As depicted in the curves of V in Figure 12, all single-mode networks exhibit stronger robustness under RA and CAR, while their robustness under CAUD and CARS remain significantly lower throughout the attack. This reveals that the connectivity, completeness, and uniformity of the networks are more severely disrupted under CAUD and CARS compared to RA and CAR when the same number of vertices are attacked. Similar trends are observed for other indicators.

The values of CR under different attack strategies demonstrate the same trend of network robustness. In any network, CR under RA and CAR is consistently higher than those under CAUD and CARS, indicating that the network can withstand more severe attacks and experience global failure at a later stage. For example, CR of the HINet under RA, CAR, CAUD, and CARS is 94.64%, 92.37%, 55.90%, and 56.36%, respectively. CR of the RINet under the four strategies is 90.54%, 84.89%, 51.42%, and 52.11%, respectively.

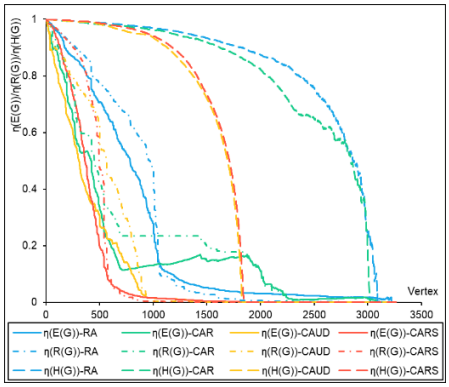

(a) HINet $\eta(E(G)_T)/\eta(R(G)_T)/\eta(H(G)_T)$

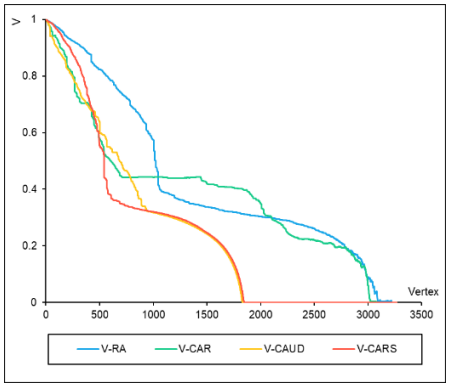

(b) HINet V

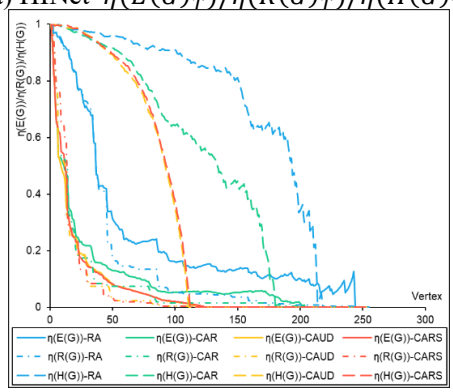

(c) RINet $\eta(E(G)_T)/\eta(R(G)_T)/\eta(H(G)_T)$

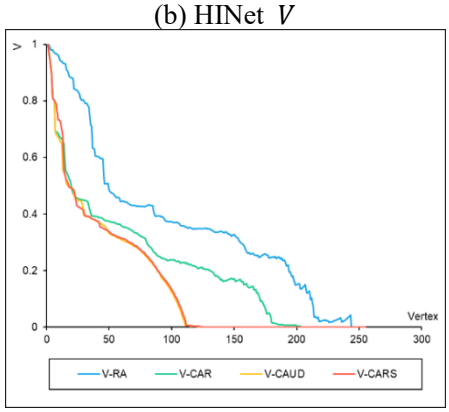

(d) RINet V

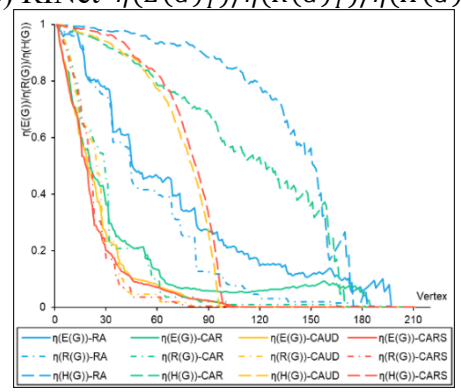

(e) NINet $\eta(E(G)_T)/\eta(R(G)_T)/\eta(H(G)_T)$

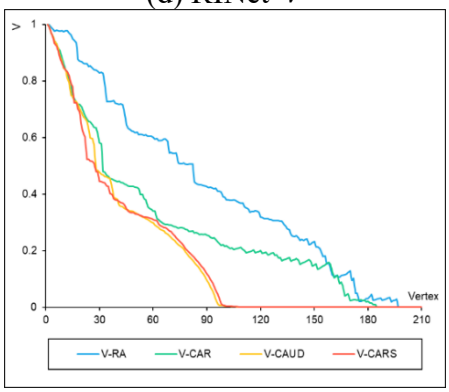

(f) NINet V

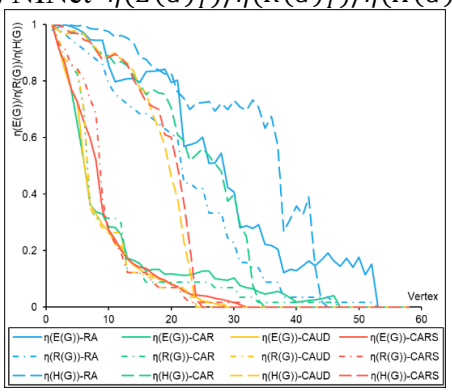

(g) AINet $\eta(E(G)_T)/\eta(R(G)_T)/\eta(H(G)_T)$

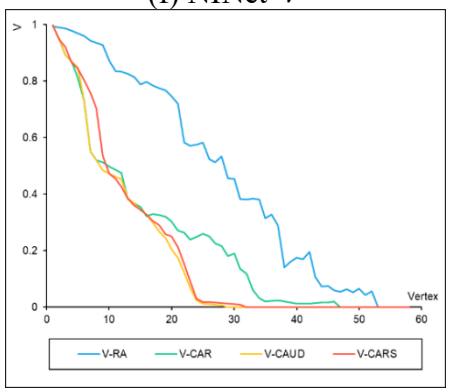

(h) AINet V

Figure 12. The robustness results of the single-mode infrastructure network.

Comparing the four networks, the HINet and RINet are more robust than the NINet and AINet, according to the speed of network failure during the entire process. The NINet and AINet experience a rapid and continuous decrease in Vthroughout the attack, revealing that their network structures are disintegrated into much smaller components more quickly. In contrast, the speed of network failure in the HINet and RINet is more complicated with three stages: the curves of V in the HINet and RINet exhibit an initial rapid decrease, follow by a fluctuation stage, and decline rapidly eventually. It indicates that the network structures of the HINet and RINet remain relatively stable at the second stage, even when a significant number of vertices are attacked.

In addition, it is found that the HINet and RINet can withstand more attacks and reach the network collapse more slowly than the NINet and AINet. The average CR of the HINet and RINet is 74.82% and 69.74%, respectively, which are higher than those of the NINet (68.01%) and AINet (66.81%).

5.2.2. Robustness comparative analysis between the CINet and single-mode infrastructure networks

Similar to the single-mode infrastructure networks, the CINet exhibits better robustness under RA and CAR than under CAUD and CARS. The CR of RA and CAR are 95.11% and 91.75%, respectively, while those of CAUD and CARS are much lower with 56.85% and 57.25%. When the network entropy decreases, the network can transit from a free and disordered state into a unified and ordered state. From the curves of structural entropy $\eta(H(G)_T)$, it is observed that the CINet better maintains its network uniformity under RA and CAR than CAUD and CARS at any period. This is reflected in Figure 13(a), where the green and blue dotted lines consistently fluctuate at a higher level for a certain period, compared to the red and yellow lines. It indicates that the network robustness under RA and CAR are prone to be stronger and can resist the transition into an ordered state.

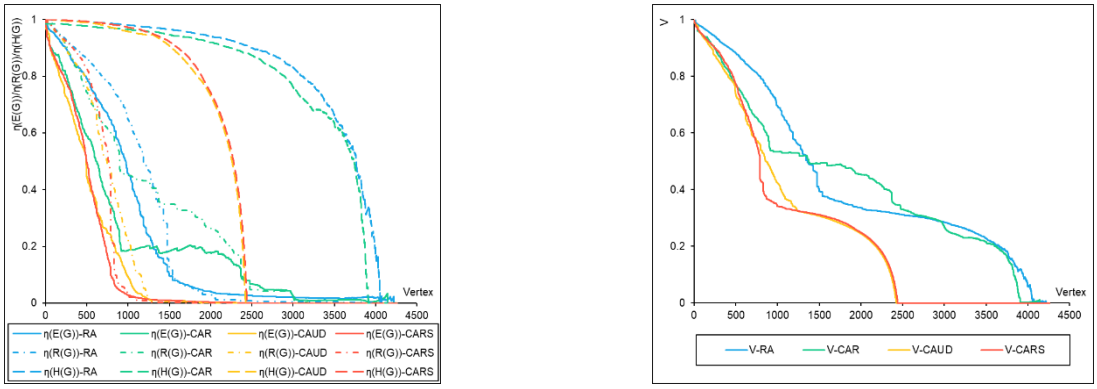

(a) $\eta(E(G)_T)/\eta(R(G)_T)/\eta(H(G)_T)$ (b) V

Figure 13. The robustness results of the CINet.

Figure 14 illustrates that the curves of the CINet and HINet are quite similar in network robustness regardless of any attack strategies and indicators. The initial E of the CINet is lower than that of the RINet, NINet, and AINet but slightly higher than that of the HINet. This phenomenon occurs because the CINet has a larger number of vertices, leading to longer average distances and lower global efficiency.

According to the trends of all indicators, it is evident that the curves of the CINet consistently remain above those of the HINet. Moreover, the HINet reaches the critical point earlier than the CINet

with a smaller CR, revealing that the CINet is more robust than the HINet.

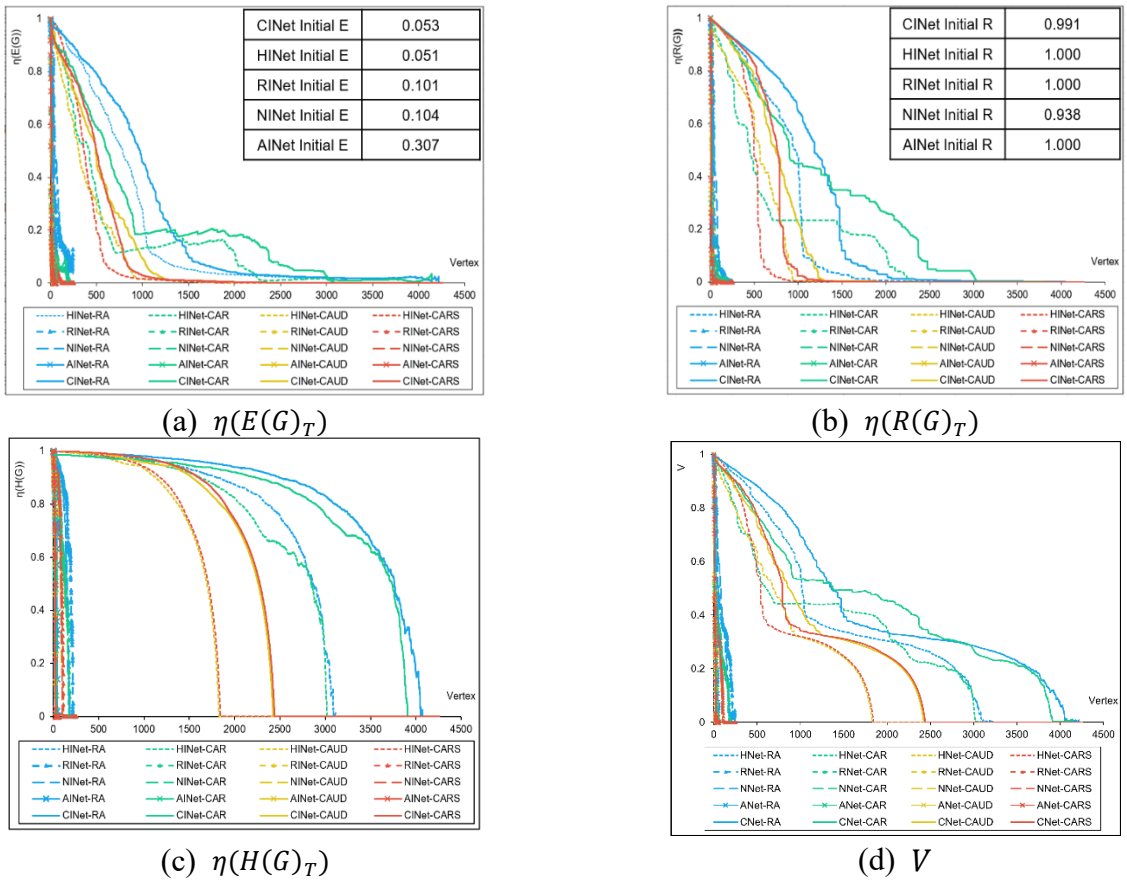

(a) $\eta(E(G)_T)$ (b) $\eta(R(G)_T)$

(c) $\eta(H(G)_T)$ (d) V

Figure 14. Robustness comparative analysis for the infrastructure network.

5.3. Robustness analysis for the operation networks

5.3.1. Robustness analysis for single-mode operation networks

Compared to the infrastructure networks, the three single-mode operation networks display similar trends under four attack strategies where the robustness under CAUD and CARS is remarkably worse than that of RA and CAR. As can be shown in Figure 15, regardless of the selected index ($\eta(E(G)_T)$, $\eta(R(G)_T)$, $\eta(H(G)_T)$, or V), the curves of CAUD and CARS consistently remain lower than that of RA. At the early stage of the attack, the trends of CAR, CARS, and CAUD show similarities until a proportion of vertices are attacked (HONet: 13%, RONet: 39%, and NONet: 20%). Then, the curves of CAR slow down, while CARS and CAUD continue to decline rapidly. In general, the single-mode operation networks are significantly more affected under CAR, CAUD, and CARS than under RA throughout the process, resulting in a worse performance on network connectivity, completeness, and uniformity.

Comparing different single-mode operation networks, it can be found that the RONet is more robust than the HONet and NONet under any attack strategy. First, the speed of network failure of the three networks is quite different. For the HONet and NONet, there is a rapid decrease in V at the initial stage and the rate of descent in the NONet is faster than that in the HONet. Then, the curve gradually declines at a low level. It reveals that the network structure is significantly disintegrated and

most of the crucial vertices are attacked during the initial stage. Conversely, the curve of the RONet witnesses a steady decline, followed by a fluctuation stage after 44–50% of the vertices are attacked, and ultimately experiences a sharp descent. This implies that the RONet demonstrates a certain level of robustness to withstand the attack in the early stages, while its connectivity, completeness, and uniformity are slightly affected.

Second, the network robustness can also be observed from CR. In the HONet, CR under RA, CAR, CAUD, and CARS is 97.10%, 46.38%, 36.71%, and 36.71%, respectively. In the RONet, CR is 97.40%, 94.81%, 74.03%, and 74.03%, respectively. While in the NONet, CR is 63.30%, 30.00%, 26.67%, and 26.67%. It is obvious that the RONet is more robust than the HONet and NONet with an average CR of 85.06%, which is higher than that of the HONet (54.23%) and NONet (36.66%). This implies that the RONet can suffer more severe attacks before collapse, while the NONet performs the worst.

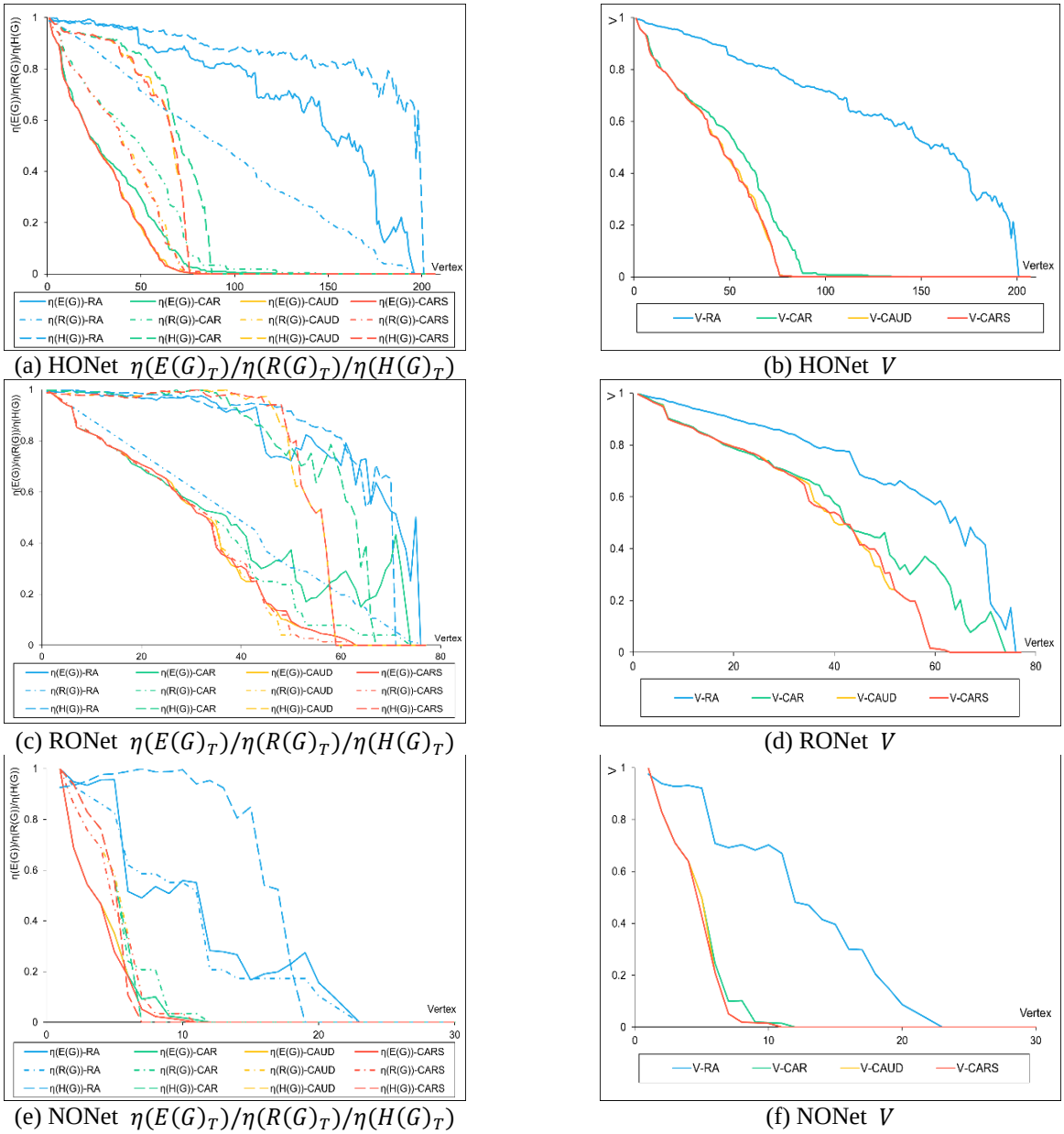

(a) HONet $\eta(E(G)_T)/\eta(R(G)_T)/\eta(H(G)_T)$ (b) HONet V

(c) RONet $\eta(E(G)_T)/\eta(R(G)_T)/\eta(H(G)_T)$ (d) RONet V

(e) NONet $\eta(E(G)_T)/\eta(R(G)_T)/\eta(H(G)_T)$ (f) NONet V

Figure 15. The robustness results of the single-mode operation network.

5.3.2. Robustness comparative analysis between the CONet and single-mode operation networks

The CONet also exhibits better robustness under RA and CAR compared to CAUD and CARS. CR under RA and CAR is 95.58% and 73.51%, respectively, which are significantly higher than CR under CAUD and CARS, which are 54.55% and 54.03%. It is noteworthy that $\eta(H(G)_T)$ first increases under CAR, CAUD, and CARS because the critical vertices (high-degree) are attacked at the initial stage and the CONet is rapidly disintegrated into several components. The network structure consequently becomes more disordered, resulting in an increase in structural entropy. Subsequently, the entropy starts to decrease and the CONet gradually converts into a more ordered state. In general, the curves of $\eta(H(G)_T)$ under RA and CAR are at a higher position compared to CAUD and CARS. This also suggests that the CONet under RA and CAR has a stronger robustness, which corresponds to the trend of the curve of V.

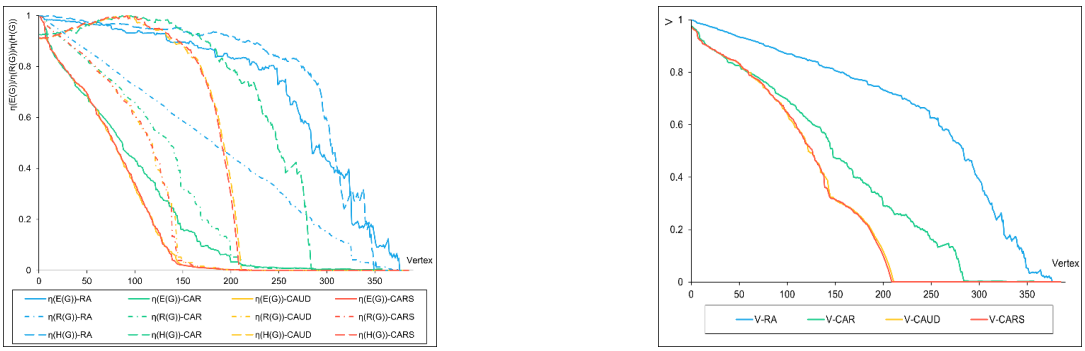

(a) $\eta(E(G)_T)/\eta(R(G)_T)/\eta(H(G)_T)$ (b) V

Figure 16. The robustness results of the CONet.

Compared to the other three single-mode operation networks, the initial $E(G)$ of the CONet is much lower because the CONet has more vertices than the others with a higher average distance.

From the curves of $\eta(E(G)_T)$, $\eta(R(G)_T)$, $\eta(H(G)_T)$, and V (Figure 17), both the CONet and the single-mode operation networks display superior robustness under RA and CAR than CAUD and CARS. This reveals that the critical vertices are more likely to be attacked under these two strategies.

The comparative analysis of different networks in CR illustrates their robustness. CR of the RONet is the highest under any attack strategy with an average value of 85.07%, indicating that the RONet has the strongest robustness among all networks. The reason for this is that each vertex in the RONet has more edges, thus generating a more concentrated network ($\bar{k} = 25.58, \bar{C} = 0.775$). Moreover, the clustering coefficients $\bar{C}$ of the other networks are all less than 0.45, and they perform worse than the RONet under attacks, with an average CR of 69.42% (CONet), 54.23% (HONet), and 36.66% (NONet), respectively.

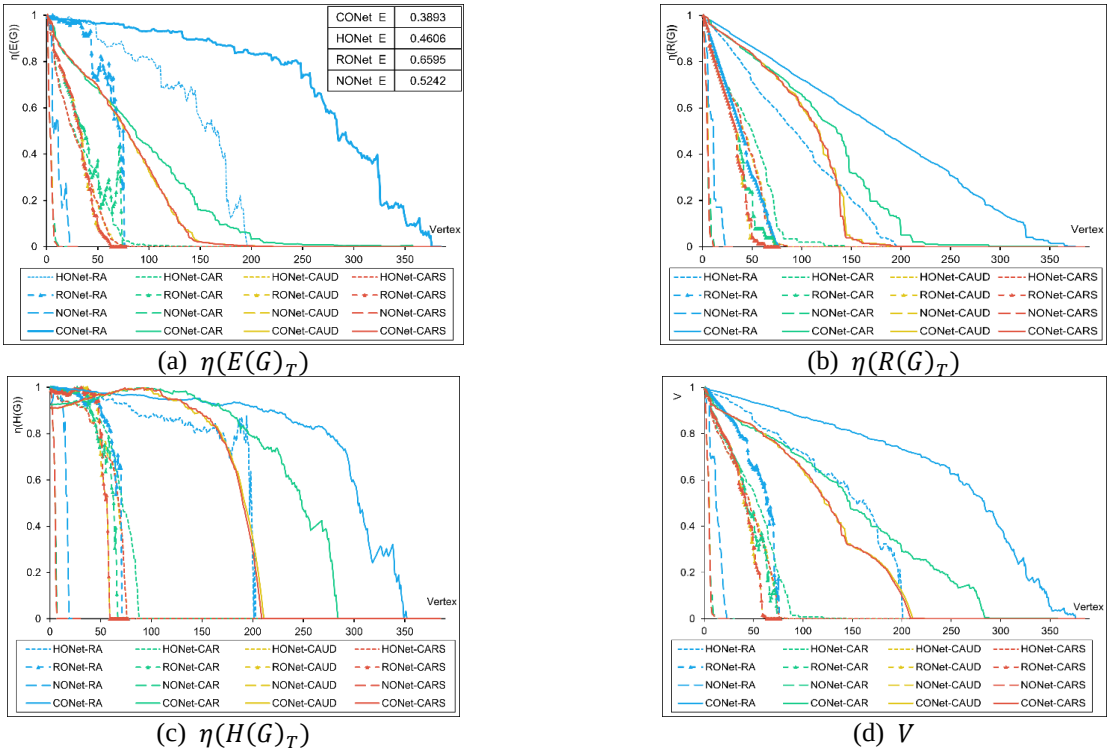

(a) $\eta(E(G)_T)$ (b) $\eta(R(G)_T)$

(c) $\eta(H(G)_T)$ (d) V

Figure 17. Robustness comparative analysis for the operation network.

5.4. Robustness comparative analysis between infrastructure networks and operation networks

5.4.1. Overall comparison of the networks' robustness

There exists a disparity in network size between infrastructure and operation networks, making it impractical to directly compare their robustness based on the curves of $\eta(E(G)_T)$, $\eta(R(G)_T)$, $\eta(H(G)_T)$, and V. On the other hand, CR depicts the proportion of the attacked vertices when the network reaches the critical point of failure. Therefore, a larger CR indicates that the network can withstand more attacks, demonstrating a stronger robustness.

From Figure 18, it is apparent that, apart from the RONet, CR of the infrastructure networks are consistently higher than those of the operation networks under any attack strategy. This implies that infrastructure networks are more robust for two reasons: 1) The edges in operation networks are operational lines. When a vertex is attacked, all associated operational lines are eliminated, leading to a rapid decline in network performance. In contrast, in infrastructure networks, the impact of a single vertex failure on robustness is limited because only the small segments directly connected to the vertex are destroyed. 2) The sizes of the operation networks are small (< 400), thereby amplifying the effect of vertex failures. Hence, when a vertex is attacked, the network reaches the critical point faster and has a lower CR.

The reason for the high robustness of the RONet is that the railway infrastructure in Jiangsu Province is well-developed. Each station operates a considerable number of railway lines. Accordingly, railway operation vertices can effectively maintain network connectivity when a single vertex is attacked.

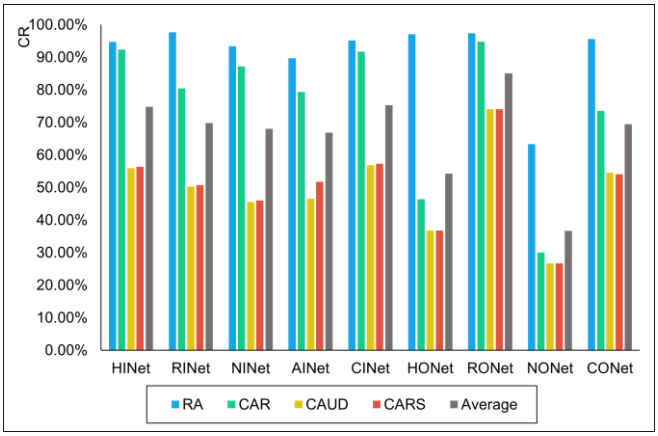

Figure 18. CR of different mode operation networks under different attack strategies.

5.4.2. Analysis of the effect of a hub attacked in the CINet and CONet

To further investigate the impact of the hub failures in the infrastructure network and operation network, a comparative experiment of attacking two hub vertices with identical geographical location in the CINet and CONet, respectively, is conducted in this section (Figure 19).

(a) Nanjing South railway station in the CINet

(b) Nanjing South railway station in the CONet

Figure 19. An example of two hubs with identical geographical location.

10 pairs of hub vertices with identical geographical location in the CONet and CINet are selected for separate attacks, as shown in Figure 20. The reduction rates of $E(G), H(G), V$ before and after the hub vertex is attacked are calculated, which are denoted as $\delta E(G), \delta H(G), \delta V$. Because only a single hub is attacked at a time, the reduction rate of $R(G)$ is not considered, and $\delta V = \frac{\delta E(G)}{2} + \frac{\delta H(G)}{2}$. The results in Figure 22 imply that $\delta E(G), \delta H(G), \delta V$ of the CONet are all larger than those of the CINet regardless of any vertex. It means that when the same hub is attacked, it has a relatively larger negative impact on the CONet compared to the CINet. This is due to the fact that the operation vertices in the CONet are directly connected, generating operational lines. Thus, the hub accommodates a substantial number of different modes of operational lines. In contrast, the CINet only considers the transfer connections at the hubs for different directions.

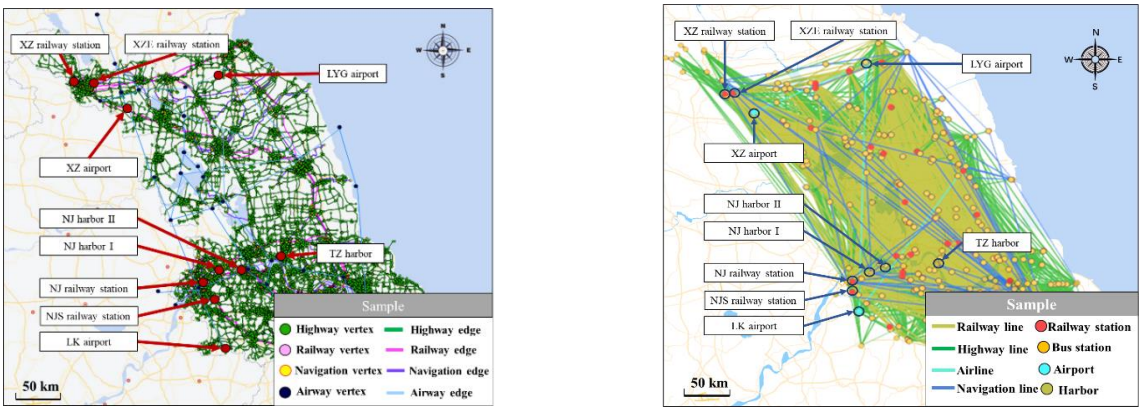

(a) 10 selected verteices in the CINet

(b) 10 selected vertices in the CONet

Figure 20. 10 pairs of selected hubs with identical geographical location.

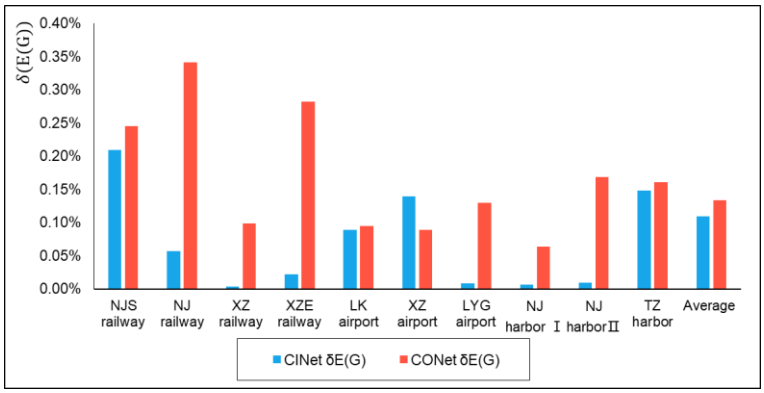

(a) $\delta E(G)$ of hub vertices in the CINet and CONet

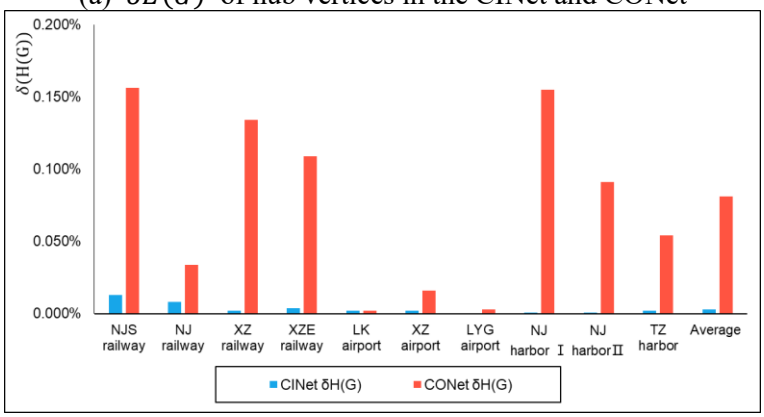

(b) $\delta H(G)$ of hub vertices in the CINet and CONet

continued on next page

Figure 21. $\delta E(G), \delta H(G), \delta V$ of different hubs in the CINet and CONet.

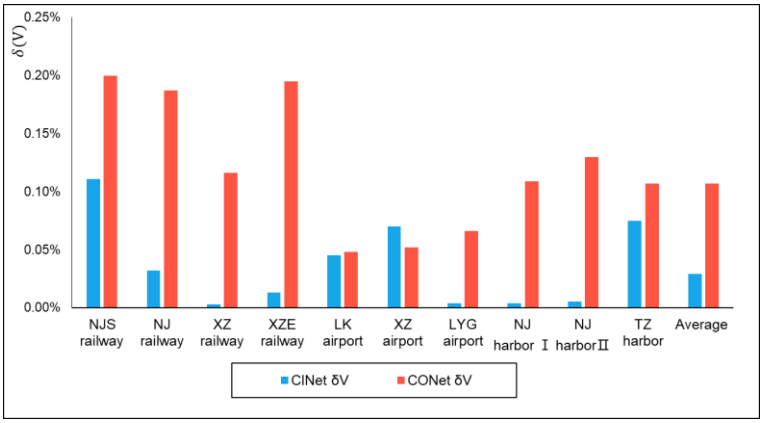

(c) δV of hub vertices in the CINet and CONet

Figure 22. $\delta E(G), \delta H(G), \delta V$ of different hubs in the CINet and CONet.

6. Discussion

In this section, four experiments are designed to explore the effect of the number of optimized hubs on the robustness of the CINet and CONet, as well as to investigate the effect of the destruction of the hubs with the same degree in the CINet on CONet. In each experiment, all networks are derived from the aforementioned data and mapping rules. For the first three experiments, comparative analyses of the robustness between the unoptimized and optimized networks are conducted. Therefore, two indicators are proposed to evaluate the robustness difference between two networks G_1 and G_2.

The improved rate of the critical ratio (IRC). This describes the change in critical rate of network failure under a certain attack strategy. It can reflect changes in robustness without being affected by network size.

$$CR^R = \frac{CP^R}{N(G)} = \frac{\varphi(R(G) = 1/100R(G)^0)}{N(G)} \tag{14}$$

$$IRC = \frac{CR_1^R - CR_2^R}{CR_2^R} \times 100\% \tag{15}$$

Similar to CR in Eq (12), CR^R refers to the critical ratio of $R(G)$ when network collapse occurs. CR_1^R and CR_2^R denote the critical ratios of G_1 and G_2, respectively. If $IRC > 0$, the robustness of G_1 is better than that of G_2.

The improved rate of $R(G)$ (IRR). This describes the average difference in $R(G)$ between two networks before network collapse. It can reflect the differences in connectivity between G_1 and G_2 when the same number of vertices have been attacked.

$$\delta^j = \frac{(R(G_1)_j - R(G_2)_j)}{R(G_2)_j} \tag{16}$$

$$IRR = \frac{\sum_j^{\min(N_1^P, N_2^P)} \delta^j}{\min(N_1^P, N_2^P)} \times 100\% \tag{17}$$

where $R(G_1)_j$ and $R(G_2)_j$ refer to $R(G)$ of G_1 and G_2 when j vertices are attacked,

respectively. δ^j is the improved rate of $R(G)$ when j vertices are attacked. If $IRR > 0$, the robustness of G_1 is better than that of G_2.

6.1. Influence of the number of optimized hubs on CINet robustness

As one of the most critical components in multimodal transportation network modeling, optimized transit hubs in the CINet are designed to represent the transfers and connections between different transportation modes. In contrast to conventional multimodal network construction methods, the design of optimized transit hubs enables a more accurate abstraction of the real-world transportation system. However, can this design effectively enhance the robustness of the CINet? This experiment is conducted to answer the question.

Two kinds of networks are constructed in this experiment: the UOCINet (unoptimized comprehensive infrastructure network) and POCINet (partially optimized comprehensive infrastructure network).

The UOCINet refers to the CINet with no optimized transit hubs where it only uses one vertex to represent the hub [24,25]. The transfer and connecting sections of the hub are not considered, while the urban high-grade edges are directly connected to the hub. The hub in the UOCINet is shown in Figure 23(b).

The POCINet denotes that only some transit hubs in the UOCINet are optimized. Optimization refers to the construction of transfer connections inside and outside the transit hub, as shown in Figure 23(a). The POCINet reflects the phenomenon that the construction resources are limited and only part of the hubs in the network can be optimized. Therefore, this experiment demonstrates the impact of the number of optimized hubs on CINet robustness, providing critical insights into the relationship between optimization scale and system resilience.

In this experiment, the POCINet is modeled by randomly selecting different proportions of transit hubs in the UOCINet to optimize. There are 211 transit hubs in the UOCINet in total. Therefore, we design 10 groups of experiments to explore the effect of the number of optimized transit hubs on the robustness of the CINet.

In each group, we randomly select α of all the transit hubs in the CINet to optimize, where $\alpha = 10\%, 20\%, \ldots, 100\%$. To eliminate the uncertainty of random selection, 10 parallel experiments are conducted for each group. The average values of IRC and IRR from the 10 parallel experiments are calculated, respectively, and regarded as the result of this group. It is worth noting that the POCINet and CINet are the same when $\alpha = 100\%$.

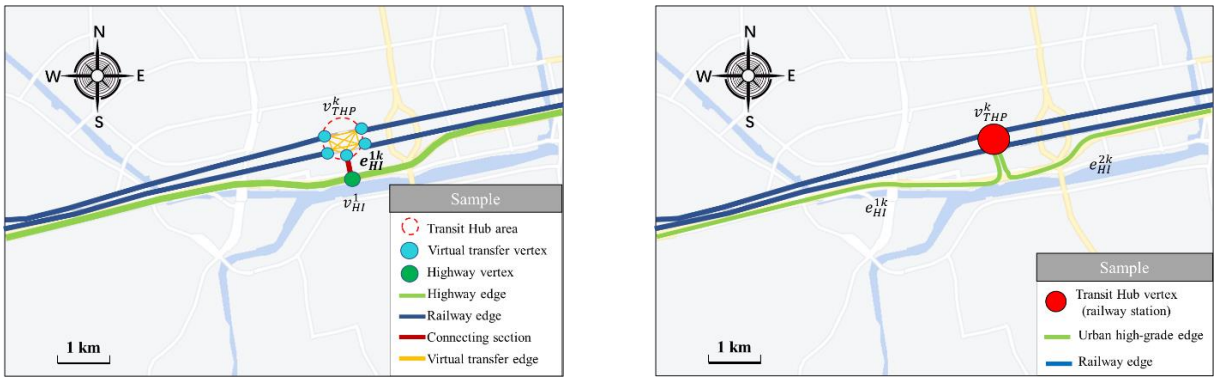

(a) Optimized hub in the POCINet (b) Unoptimized hub in the UOCINet

Figure 23. Difference between the optimized and unoptimized transit hub when modeling.

Table 3 and Figure 24 display that IRC and IRR remain positive across different values of α under different strategies, indicating that the optimization of the hubs enhances the network robustness. With the increase in α, IRR shows a steadily increasing trend from 17.05% to 114.56%. At the same time, IRC fluctuates between 1.78% and 4.55%. However, IRC and IRR vary under different attack strategies. Under CAR, CAUD, and CARS, IRC and IRR show a progressive increase with increasing α. In contrast, under RA, both of them exhibit notable fluctuations where IRC is even less than zero and IRR fluctuates by nearly 30%, as illustrated in Figure 24. Furthermore, this fluctuation can be more prominently observed in Figure 25(a) where the curves of δ^j under RA exhibit irregular fluctuations across different α. For example, when $\alpha = 90\%$, the curve fluctuates wildly between 0–180%. However, in Figure 25(b)–(d), all the curves display a relatively consistent pattern of fluctuations, and the larger α is, the higher the corresponding curve is.

Table 3. IRC and IRR between the POCINet and UOCINet.

α	RA			CAR			CAUD			CARS			Average values of four attacks	
POCINet	CR^R/%	IRC/%	IRR/%	CR^R/%	IRC/%	IRR/%	CR^R/%	IRC/%	IRR/%	CR^R/%	IRC/%	IRR/%	IRC/%	IRR/%
UOCINet	56.31	0	0	73.44	0	0	29.55	0	0	26.06	0	0	0	0
10%	58.99	4.76	23.54	73.77	0.45	14.87	29.67	0.40	3.08	26.45	1.49	26.71	1.78	17.05
20%	60.55	7.54	30.86	73.81	0.50	16.75	29.95	1.36	9.44	26.70	2.46	40.89	2.96	24.48
30%	58.02	3.05	22.67	74.31	1.18	32.19	30.11	1.88	13.18	26.54	1.84	39.56	1.99	26.90
40%	58.84	4.50	40.67	74.53	1.48	35.98	30.20	2.19	21.57	26.36	1.14	71.27	2.33	42.37
50%	58.60	4.07	38.17	74.67	1.67	56.70	30.35	2.69	26.03	26.77	2.71	79.49	2.78	50.10
60%	55.22	-1.93	26.87	74.97	2.08	68.72	30.69	3.85	39.52	27.02	3.68	115.59	1.92	62.68
70%	57.91	2.84	32.92	75.35	2.61	88.61	30.63	3.64	41.32	27.08	3.91	151.08	3.25	78.48
80%	55.79	-0.92	31.25	75.31	2.54	96.13	30.78	4.14	47.96	26.77	2.73	162.62	2.12	84.49
90%	56.15	-0.28	38.40	76.27	3.85	126.77	31.09	5.20	63.61	26.77	2.73	169.57	2.88	99.59
100% (CINet)	57.02	1.31	42.45	76.26	3.84	146.72	31.12	5.29	73.77	28.09	7.79	195.30	4.55	114.56

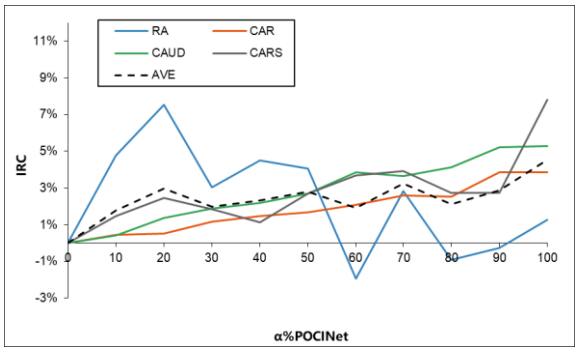

(a) IRC

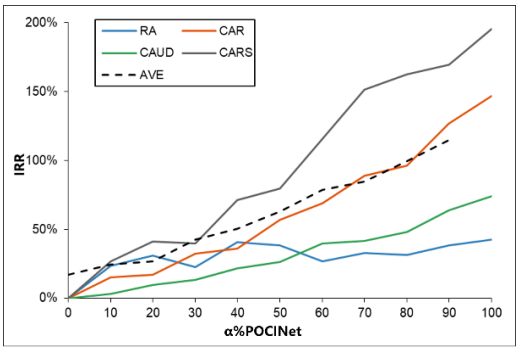

(b) IRR

Figure 24. Changes in IRC and IRR with different α of the POCINet.

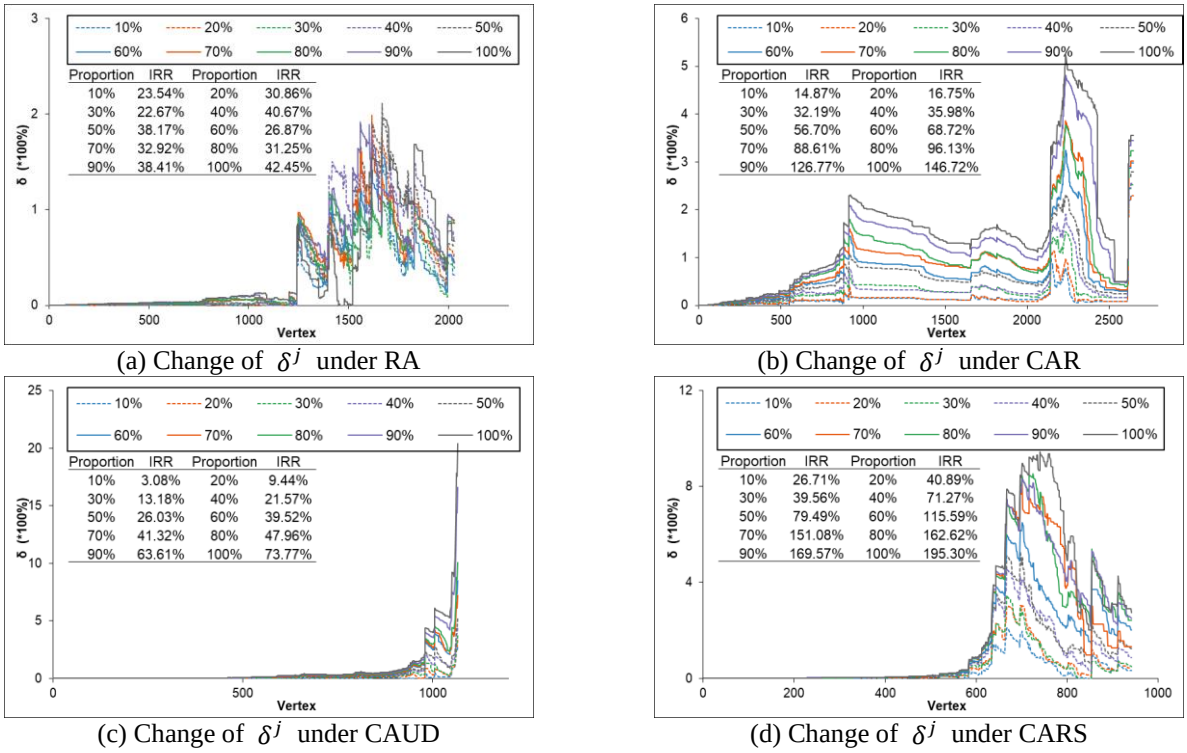

(a) Change of δ^j under RA

(b) Change of δ^j under CAR

(c) Change of δ^j under CAUD

(d) Change of δ^j under CARS

Figure 25. Change of δ^j with different α.

It is evident that the POCINet demonstrates greater robustness than the UOCINet, thereby reflecting the effectiveness of our proposed optimization design in network resilience enhancement. Compared to random attacks, the improvement is more pronounced under calculated attacks. Meanwhile, the network robustness exhibits continuous improvement under calculated attacks when more transit hubs are optimized (α increases). In contrast, the effect of robustness improvement still fluctuates at a lower level under random attacks.

Compared to traditional modeling methods, the optimized design of transit hubs can effectively enhance the robustness of the CINet for the following two reasons:

1) Increase in the number of vertices. The optimized design method proposed in this paper reflects the internal and external connections of transit hubs, splitting the original single hub of the traditional modeling method into a local network of transit hubs composed of multiple virtual vertices and edges. Essentially, this method directly increases the number of vertices in the network, resulting in a more tightly connected network with a higher clustering coefficient. Consequently, the network's ability to withstand external attacks is enhanced and its robustness is effectively improved.

2) Improvement in the transfer ability of the transit hub. After utilizing the optimized design of transit hubs, the network indeed experiences an increase in the number of vertices. However, the new vertices are not distributed randomly in the network but are strategically added at the transit hubs. The existence of these vertices strengthens the connections between different transportation modes of the transit hub, thereby enhancing its transfer ability. Compared to the traditional modeling methods, the improvement in the hub's transfer ability can optimize the network robustness under external disturbances. For example, when a transit hub is attacked and some of its channels need to be closed, the traditional modeling method would remove the entire hub vertex and its connecting edges from the network, resulting in a rapid decomposition of network structure. In contrast, under the optimized design, only the closed transfer channels are removed, while the other components of the transit hub

can maintain normal operation. This effectively preserves the network robustness.

From a practical aspect, compared to the traditional multimodal network construction methods, the optimized transit hubs in the CINet contribute to the network's ability to withstand external disturbances. This suggests that the construction of internal transfer channels and external connections of the transit hubs are necessary. The internal transfer channels' design not only depicts the transfer process between different transportation modes, but also achieves the physical separation of different directions. This ensures that the failure of a single channel does not affect the normal operation of other parts of the transit hub, and effectively enhances the network robustness. The external connections' design can avoid the direct connection between the high-grade roads and the hub, which mitigates heavy traffic loads on the hub and effectively optimizes its traffic organization and management.

6.2. Influence of the number of optimized hubs on CONet robustness

In this section, two networks–UOCONet (unoptimized comprehensive operation network) and POCONet (partially optimized comprehensive operation network) are applied to clarify the effect of the number of optimized hubs on CONet robustness. The hubs in the CONet refer to the vertices that possess multiple modes of operational lines, and there are only 55 hub vertices in the CONet.

UOCONet refers to the CONet with no optimized hubs where it only uses one vertex to represent the hub, and the connections to other intra-city vertices of the hub are not considered. The hub in the UOCONet is shown in Figure 26(b). POCONet means that only some hubs in the UOCONet are optimized. Optimization refers to the construction of a mode transfer network inside the hub and a connection network outside the hub, as shown in Figure 26(a).

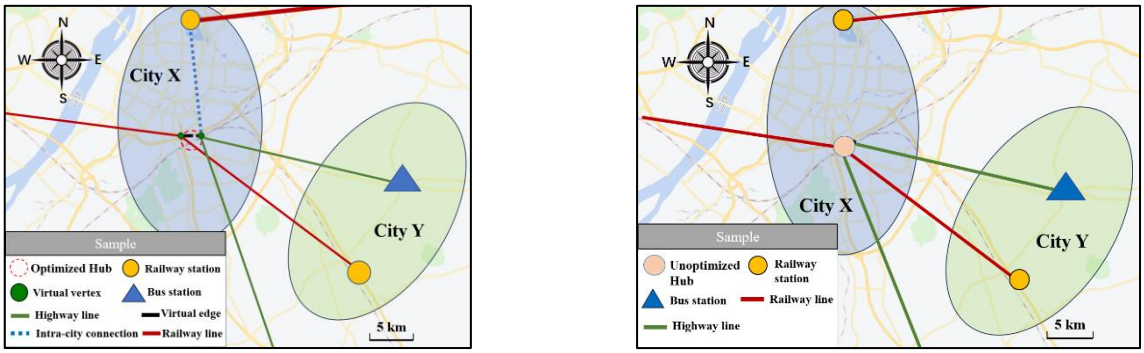

(a) Optimized hub in the POCONet

(b) Unoptimized hub in the UOCONet

Figure 26. Difference between the optimized and unoptimized hub when modeling.

The experiment conducted in this section is similar to that in Section 6.1. 55 hub vertices are selected randomly according to the selection proportion α, ranging from 10% to 100%. 10 parallel experiments are conducted for each group, and the average values of IRC and IRR of 10 parallel experiments are calculated, respectively, and regarded as the result of this group.

Table 4. IRC and IRR between the POCONet and UOCONet.

α POCONet	RA			CAR			CAUD			CARS			Average values of four attacks	
	CR^R/%	IRC/%	IRR/%	CR^R/%	IRC/%	IRR/%	CR^R/%	IRC/%	IRR/%	CR^R/%	IRC/%	IRR/%	IRC/%	IRR/%
UOCONet	56.32	0	0	62.11	0	0	37.82	0	0	34.47	0	0	0	0
10%	58.81	0.87	31.42	62.25	0.23	11.23	37.99	0.45	10.48	34.73	0.75	19.17	0.57	18.075
20%	55.23	-1.94	26.87	62.85	1.19	15.49	38.17	0.93	16.94	35.02	1.60	34.19	0.44	23.37
30%	55.77	-0.98	27.95	62.77	1.06	28.67	38.36	1.43	27.37	35.17	2.03	58.24	0.89	35.56
40%	54.92	-2.49	34.66	63.19	1.74	39.44	38.29	1.24	33.19	35.36	2.58	77.73	0.77	46.26
50%	57.54	2.17	38.47	63.34	1.98	52.75	38.75	2.46	40.63	35.09	1.80	92.28	2.10	56.03
60%	58.78	4.37	30.16	63.28	1.88	70.01	38.91	2.88	45.56	35.55	3.13	113.54	3.07	64.82
70%	56.22	-0.18	29.41	63.86	2.82	83.47	39.24	3.75	51.28	35.83	3.95	132.65	2.59	74.20
80%	57.61	2.29	35.74	64.1	3.2	102.31	39.36	4.07	56.72	35.96	4.32	146.71	3.47	85.37
90%	58.88	4.55	38.4	64.03	3.09	114.42	39.11	3.41	60.61	36.14	4.84	155.84	3.97	92.32
100% (CONet)	58.63	4.10	39.97	63.97	2.99	126.18	39.43	4.26	67.38	36.21	5.05	163.41	4.10	99.24

Table 4 and Figure 27 show that the effect of the number of optimized hubs in the CONet is similar to that in the CINet. IRC and IRR are generally positive under the four attack strategies. An upward trend from 18.08% to 99.24% can be observed in IRR with the increasing number of optimized hubs, while IRC fluctuates between 0.57% and 4.10% at the same time. Besides, the trends of IRC and IRR differ under various attack strategies. The effect under RA is the worst as both IRC and IRR exhibit fluctuations by 6.86% and 13%, respectively. Moreover, under CAR, CAUD, and CARS, IRC and IRR gradually increase with increasing α, indicating that the optimized hub vertices can enhance the robustness of the CONet.

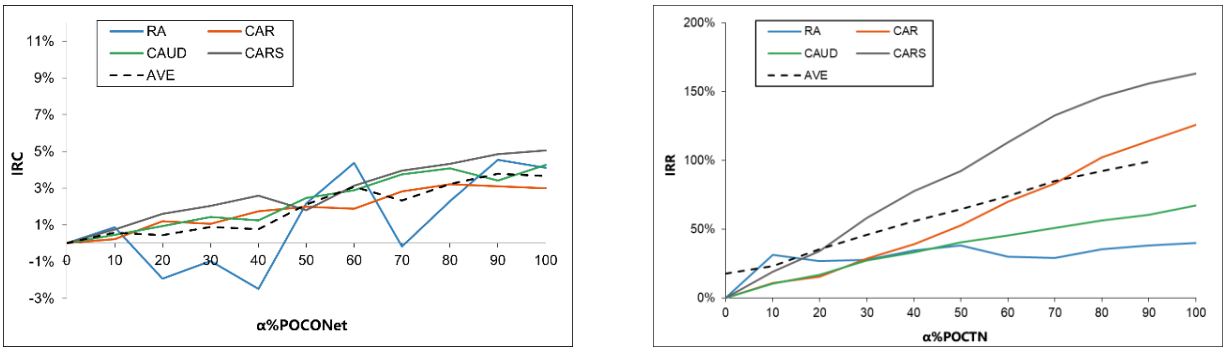

(a) IRC (b) IRR

Figure 27. Changes in IRC and IRR with different α of the POCONet.

The results reveal that the optimized design of the hubs can effectively improve the robustness of the CONet. The enhancement is more significant as the number of optimized hubs increases. The reasons for this improvement in the CONet are mainly attributed to the following three points:

1) Increase in the number of vertices and connections. Similar to the transit hubs in the CINet, the design of the operation hub in the CONet also increases the number of the vertices and connections. In addition, the number of connections between the operation hub and other intra-city operation vertices is also significantly increased. The growth in network scale leads to a more densely

interconnected network structure, which improves its ability to withstand external attacks.

2) The construction of the connection network of intra-city operation vertices. Compared to traditional modeling methods in previous studies, the intra-city connection network strengthens the connections between the operation hub and other operation vertices within the city. Additionally, since the operation hubs are high-class vertices, they can generate a large number of intra-city connections, thereby enhancing connectivity among operation vertices within the same city. In other words, it is considered that the vertices within each city form a tightly connected cluster of the network to some extent. As a result, the CONet is less likely to be disintegrated under attacks, and the network robustness is effectively improved.

3) Mode transfer design of the operation hub. The mode transfer design decomposes the operation hub into different modes of virtual transfer vertices and edges. When the hub is under external disturbances, if the operational lines of one mode are disrupted, the other modes of lines remain unaffected. For example, Shanghai Hongqiao International Airport is an operation hub integrating three transportation modes: highway, railway, and aviation. When severe weather events such as strong winds occur, all flights may be suspended, but the railway and highway lines can continue to operate normally. Therefore, only the aviation virtual vertices and their connected edges need to be removed while the lines of highway and railway can still operate normally. Consequently, the network with optimized design can withstand more attacks than the network constructed by traditional methods, thereby demonstrating its effect on network robustness enhancement.

From the practical perspective, it is obvious that optimized hubs can significantly enhance the network robustness and withstand calculated attacks. It suggests that in the planning and construction stage, it is necessary to construct the internal mode transfer network and the intra-city connection network of the hub. This construction can contribute to optimizing the layout of densified operational lines and enhance the connectivity among different modes of operation vertices, resulting in the network's ability to withstand external disturbances.

6.3. Effect of the optimization of hubs with identical geographical location on network robustness

As mentioned in Section 3, the CINet and CONet exhibit differences in their topological structures and modeling methods, leading to both correlations and distinctions in their robustness. In order to investigate the interactions of robustness between the CINet and CONet, we define their robustness relationships and distinctions as the robustness improvement differences which result from the optimization of the same hub vertices. Since there are some hub vertices with identical geographical location in the CINet and CONet (as depicted in Section 5.4.2), the experiments of this section will be designed based on them. By comparing the effect of the optimization of hub vertices on network robustness improvement of the CINet and CONet, this section aims to systematically analyze the interactions between the two networks.

There are 55 hub vertices in both the CINet and CONet, each of them shares the identical geographical location in these two networks. To better display their robustness relationships and distinctions, 11 groups of experiments are designed. In each group, n hub vertices are randomly selected from the 55 hub vertices, where $n = 5, 10, \ldots, 55$, with an increment of 5. The selected hub vertices are optimized in the UOCINet and UOCONet, respectively, to construct the optimized networks–POCINet and POCONet. That is, in each group, the same hub vertices are optimized in the two networks.

Based on the four attack strategies, the robustness of the networks before and after optimization are analyzed. Moreover, to eliminate the uncertainty of random selection, each group of experiments

is conducted 10 times in parallel. The average values of IRC and IRR of these 10 parallel experiments are calculated, respectively, and regarded as the result of this group.

Table 5. IRC and IRR between the POCINet and UOCINet**.**

n optimized hubs in the POCINet	RA			CAR			CAUD			CARS			Average values of four attacks	
	CR^R/%	IRC/%	IRR/%	CR^R/%	IRC/%	IRR/%	CR^R/%	IRC/%	IRR/%	CR^R/%	IRC/%	IRR/%	IRC/%	IRR/%
UOCINet	56.12	0	0	73.44	0	0	29.55	0	0	26.06	0	0	0	0
5	57.41	2.30	22.12	73.52	0.11	13.71	29.59	0.14	2.95	26.14	0.31	28.16	0.71	16.74
10	57.37	2.23	23.48	73.57	0.18	17.68	29.64	0.30	3.64	26.18	0.46	36.41	0.79	20.30
15	56.01	-0.20	25.73	73.79	0.48	23.47	29.75	0.68	8.81	26.15	0.35	39.72	0.33	24.43
20	55.86	-0.46	28.86	73.85	0.56	29.26	29.88	1.12	13.27	26.34	1.07	48.17	0.57	29.89
25	58.01	3.37	32.75	73.72	0.38	36.45	29.81	0.88	15.43	26.46	1.53	53.24	1.54	34.47
30	56.95	1.48	36.37	73.91	0.64	38.92	29.96	1.39	14.26	26.9	3.22	59.95	1.68	37.38
35	56.43	0.55	34.69	74.06	0.84	36.01	29.92	1.25	19.99	26.83	2.95	57.68	1.40	37.09
40	56.22	0.18	35.19	74.11	0.91	37.39	29.95	1.35	20.08	26.66	2.30	60.54	1.19	38.30
45	57.41	2.30	35.51	74.15	0.97	39.54	30.01	1.56	22.11	26.59	2.03	63.33	1.71	40.12
50	57.74	2.89	37.94	74.19	1.02	41.08	30.08	1.79	21.92	26.77	2.72	62.59	2.11	40.88
55	57.97	3.30	39.21	74.37	1.27	42.73	30.17	2.10	23.74	26.81	2.88	66.81	2.38	43.12

Table 6. IRC and IRR between the POCONet and UOCONet**.**

n optimized hubs in the POCONet	RA			CAR			CAUD			CARS			Average values of four attacks	
	CR^R/%	IRC/%	IRR/%	CR^R/%	IRC/%	IRR/%	CR^R/%	IRC/%	IRR/%	CR^R/%	IRC/%	IRR/%	IRC/%	IRR/%
UOCONet	55.97	0	0	62.11	0	0	37.82	0	0	34.47	0	0	0	0
5	56.21	0.43	29.77	62.48	0.60	12.13	38.01	0.50	10.62	34.79	0.93	19.23	0.61	17.94
10	55.37	-1.07	30.01	62.79	1.09	15.21	38.14	0.85	14.97	34.98	1.48	33.74	0.59	23.48
15	56.02	0.09	28.55	62.82	1.14	31.48	38.33	1.35	27.44	35.14	1.94	56.19	1.13	35.92
20	55.04	-1.66	32.71	63.21	1.77	39.46	38.32	1.32	35.14	35.28	2.35	78.07	0.95	46.35
25	57.26	2.30	35.43	63.38	2.04	51.97	38.81	2.62	40.01	35.31	2.44	90.46	2.35	54.47
30	58.24	4.06	34.98	63.47	2.19	71.11	38.91	2.88	45.54	35.53	3.08	113.28	3.05	66.23
35	57.75	3.18	32.64	63.78	2.69	81.35	39.24	3.75	51.36	35.91	4.18	134.85	3.45	75.05
40	56.53	1.00	32.87	64.09	3.19	92.54	38.85	2.72	54.25	35.99	4.41	140.01	2.83	79.92
45	57.41	2.57	33.09	64.15	3.28	100.09	39.37	4.10	56.73	36.03	4.53	146.63	3.62	84.14
50	58.78	5.02	37.16	64.11	3.22	114.72	39.13	3.46	61.01	36.12	4.79	158.32	4.12	92.80
55	58.59	4.68	39.22	63.97	2.99	126.18	39.43	4.26	67.38	36.21	5.05	163.41	4.25	99.05

Table 5 and 6 depict the IRC and IRR of the CINet and CONet. It is evident that as the number of optimized hub vertices increases, both the CINet and CONet exhibit an upward trend in IRC, with the CINet eventually increasing to 2.38% and the CONet increasing to 4.25%. It indicates that when optimizing the same hub vertices, the CONet can withstand more severe attacks before reaching the critical point of network collapse compared to the CINet. IRR further displays a more significant

result that it increases from 16.74% to 43.12% in the CINet, whereas it rises from 17.94% to 99.05% in the CONet. It implies that as the number of optimized hub vertices increases, the robustness enhancement is more pronounced in the CONet than in the CINet.

Figure 28 provides a more intuitive comparison of the robustness improvement between the CINet and CONet under the optimization of the hub vertices with identical geographical location. It is clear that the solid lines representing IRC of the CONet consistently lie above the dashed lines representing IRC of the CINet under the three calculated attack strategies. Under random attacks, the CINet initially exhibits a higher IRC, fluctuating between -0.46% and 3.37%, while the CONet fluctuates between -1.66% and 2.3%. However, when more than 25 hub vertices are optimized, the IRC of the CONet is larger than that of the CINet. A similar pattern is observed in Figure 28(b), where the IRR of the CONet is significantly higher than that of the CINet under calculated attack strategies, but both of them are comparable under random attacks.

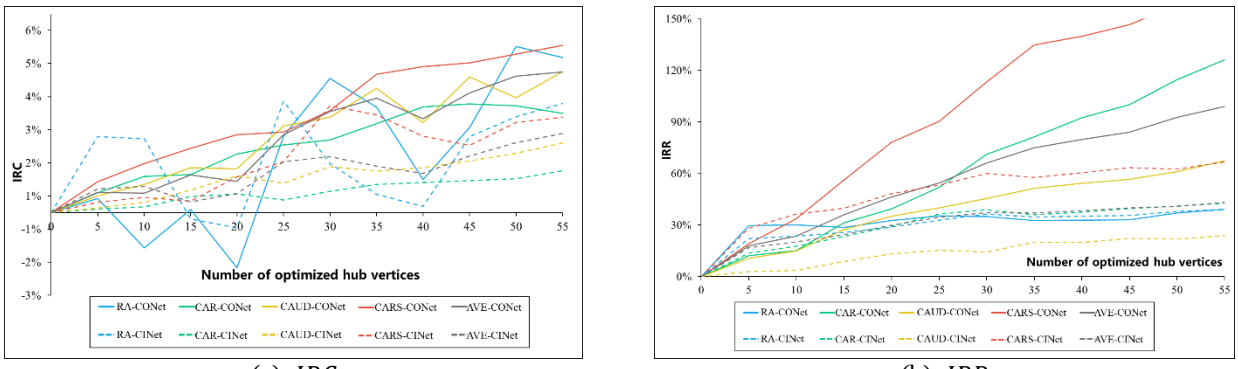

(a) IRC (b) IRR

Figure 28. Changes in IRC and IRR with different numbers of optimized hubs.

The results indicate that the effect of the optimization of the hub vertices with identical geographical location on robustness enhancement is more pronounced in the CONet than in the CINet, particularly under calculated attacks. In contrast, under random attacks, the robustness enhancement of the two networks exhibits similar performance with certain fluctuations.

When optimizing the hub vertices with an identical geographical location, the reasons for the differences in the robustness enhancement between the CINet and CONet are as follows:

1) Network scale. The network scale of the CINet is significantly larger than that of the CONet. Specifically, the CINet contains 4046 ordinary vertices and 211 hub vertices, while the CONet has 330 ordinary vertices and 55 hub vertices, which reveals that the hub vertices in the CONet possess more connections. Therefore, from a quantitative perspective, hub vertices play a more critical role in the CONet. Consequently, when optimizing the same hub vertex (such as Nanjing South railway station), the growth rate of the vertex quantity in the CONet is 0.52%, whereas that in the CINet is only 0.12%. This results in a more pronounced improvement in network robustness of the CONet compared to the CINet.

2) Number of connections generated by the optimized hub design. When optimizing the hubs, a large number of new connections are generated. In the CINet, the new connections primarily include virtual edges between different transfer channels within the hub and external connections of the hub. In contrast, in the CONet, the new connections consist of virtual edges for mode conversion within the hub and external connections linking to other intra-city operation vertices. Since there are numerous operation vertices in a city and the hub vertex often has a higher class, a substantial number of

connections between them are established accordingly. As a result, when optimizing the same hub vertex, there are more new connections in the CONet compared to the CINet, leading to a more pronounced enhancement in the robustness of the CONet.

Therefore, in the context of transportation management, optimizing the operation line planning of hub vertices is more beneficial for network robustness improvement compared to the optimization of the infrastructure construction of hub vertices. This suggests that, when under existing transportation infrastructure and cost limitations, prioritizing the optimization of hub vertices in the CONet is more effective in the robustness enhancement of regional transportation systems, compared to optimizing those in the CINet.

6.4. *Effect of the destruction of different hubs with the same degree in the CINet on CONet*

The comprehensive operation network (CONet) is constructed based on the comprehensive infrastructure network (CINet). Although some hubs in the CINet share the same scale, same class, and similar functions, they may operate a different number of lines in the CONet, leading to variations in their operational roles. Hence, the following questions are raised: How does the failure of the hubs with the same degree in the CINet but different degrees in the CONet affect the robustness of the CONet? What are the differences in their impacts? These questions will be addressed in this section.

A total of eight hub vertices in the CINet are selected and divided into three groups for experimental analysis, and the vertices in each group share the same scale (or class). Each vertex is attacked individually, and the reduction rates $\delta E(G), \delta H(G), \delta R(G), \delta V$ are calculated. Because only one vertex is attacked at a time, the $\delta R(G)$ of each vertex is the same.

The results reveal that for the hub vertices of the same scale in the CINet, those with higher degrees in the CONet manage more operational lines and are more vulnerable to attacks, resulting in significant impacts on network robustness. For example, Huai'an, Wuxi East, and Yangzhou railway stations are second-class stations and have a vertex degree of 3 in the CINet. When attacked, δV of Yangzhou railway station is the largest (0.151%) with a degree of 28 in the CONet, while the δV of Huai'an and Wuxi East are 0.122% and 0.135%, respectively.

Table 7. $\delta E(G), \delta H(G), \delta R(G), \delta V$ of the vertices with the same degree in the CINet.

Group	Name	Class	CINet $\bar{k}$	CONet $\bar{k}$	$\delta E(G)$	$\delta R(G)$	$\delta H(G)$	δV
1	Xuzhou airport	4D airport	3	11	0.089%	0.26%	0.016%	0.121%
	Lianyungang airport	4D airport	3	13	0.130%	0.26%	0.003%	0.131%
2	Wuxi South railway station	top-class	5	18	0.006%	0.26%	0.071%	0.112%
	Changzhou railway station	top-class	5	48	0.193%	0.26%	0.084%	0.179%
	Xuzhou East railway station	top-class	5	57	0.282%	0.26%	0.109%	0.217%
3	Huai'an railway station	class II	3	13	0.024%	0.26%	0.080%	0.122%
	Wuxi East railway station	class II	3	14	0.049%	0.26%	0.095%	0.135%
	Yangzhou railway station	class II	3	28	0.074%	0.26%	0.119%	0.151%

The reasons for the difference in the impact on robustness of different hub failures are as follows:

1) Distribution of other hub vertices within the same city. Although some hub vertices are of the same scale in the CINet, their operational roles differ due to the cities they are located in and the distribution of other hub vertices within the same city. For example, in Group 2, Wuxi South railway station is located in a city (Wuxi) with three other railway stations (Wuxi station, Wuxi-xinqu station, and Wuxi East station), whereas Changzhou and Xuzhou East railway station each have only one another station within their respective cities (Changzhou North station and Xuzhou station). As a result, the operational lines in Wuxi are distributed by multiple stations, leading to fewer lines being handled by Wuxi South railway station compared to the other two hub vertices of the same scale. Therefore, although the three hub vertices in Group 2 have comparable infrastructure facilities, Changzhou and Xuzhou East railway station manage a greater number of operational lines, and their failures would have a more significant impact on the robustness and operation of the CONet. The same analytical reasoning applies to Group 3.

2) Geographical location. In Group 3, the number of operational lines in Wuxi East and Huai'an railway stations are comparable (13 and 14, respectively), and Wuxi East station even has more other hub vertices within the same city. However, the failure of Wuxi East station has a greater impact on the robustness of the CONet, which can be primarily attributed to geographical location. Since Wuxi East station is located in the southern part of Jiangsu Province, its infrastructure development and transportation functions are more advanced compared to Huai'an, which is situated in the northern part of Jiangsu. As a result, Wuxi East station is connected to more critical operation vertices. From the network perspective, its failure can cause a more significant impact on the network robustness of the CONet, compared to Huai'an station. A similar situation applies to the two airports in Group 1.

The findings suggest that balancing the operational lines of each hub vertex is necessary for the construction of the CONet. It helps decentralize high-degree hub vertices into multiple smaller hubs, thereby reducing the negative impact on the overall network robustness caused by the attacks on high-degree hub vertices.

7. Conclusions

The CTN exhibits a complex topological structure and various basic elements, playing a critical role in regional transportation operation and economy development. In order to thoroughly investigate the comprehensive transportation system, this paper divides the CTN into two perspectives: the CINet and CONet, with optimized modeling methods. Specifically, the optimized designs of the hubs in the CINet and CONet are meticulously considered. Subsequently, Jiangsu Province is taken as a case study to analyze the network statistical characteristics and robustness, offering valuable insights for transportation planning and management. The main conclusions of this paper can be summarized as follows:

1) Robustness comparative analyses are conducted among multi-mode infrastructure networks and operation networks. It is found that the CINet exhibits the highest robustness compared to the other four single-mode infrastructure networks. However, the RONet exhibits the best robustness among all the operation networks. All networks possess a certain level of robustness against external disturbances under different attack strategies, and they demonstrate superior robustness under RA and CAR compared to CAUD and CARS.

2) Differences in the robustness between the operation networks and infrastructure networks are analyzed. We find that operation networks demonstrate weaker robustness than the infrastructure

networks, particularly under any calculated attack strategy, as indicated by their smaller CR values. Additionally, when two hubs with identical geographical location in the CINet and CONet are attacked simultaneously, the negative impact on the robustness of the CONet is greater than on the CINet, implying that hubs in the CONet play a more critical role in network connectivity.

3) The effect of optimized hub designs on network robustness improvement is quantitatively investigated. We find that the optimized designs significantly enhance the network robustness, especially under calculated attacks. For the CINet, the average critical rate of network failure (IRC) is delayed by 4.55% and the average rate of connectivity improvement (IRR) reaches 114.56%, compared to the UOCINet without optimized hubs. For the CONet, IRC and IRR are 4.10% and 99.24%, respectively, compared to the UOCONet. This indicates that both the CINet and CONet can be more robust as the number of optimized hub vertices increases. This highlights the importance and effectiveness of optimized hubs in mitigating the impact of external attacks on network robustness.

4) The interactions between the robustness of the CINet and CONet are analyzed. When optimizing the hub vertices with identical geographical location in the CINet and CONet, we find that the effect of the optimization on network robustness enhancement is more pronounced in the CONet compared to the CINet. Specifically, the CONet exhibits an IRC of 4.25% and an IRR of 99.05%, whereas those of the CINet are 2.38% and 43.12%, respectively. This reveals that the CONet is more sensitive to the optimization of hub vertices and that its network robustness improvement is more effective than that of the CINet. This highlights the importance that optimizing the operation networks, rather than constructing the infrastructure networks, has greater engineering significance in enhancing the robustness of transportation systems under cost limitations.

5) The impact of the failure of different hubs with the same degree on the CONet is comparatively explored. When several hub vertices with the same scale in the CINet but of different degrees in the CONet are attacked, the higher the degree of a vertex in the CONet, the greater the damage to the CONet after its failure. This implies that when hubs in the CINet are of comparable scale, the planning of operational lines should be distributed in balance among these hubs. In this way, all hub vertices in the CONet can possess comparable operational lines, enabling the network to better distribute the traffic load and minimize the impact on robustness when high-degree vertices in the CONet fail.

According to the research results above, we provide the following suggestions. 1) In the planning stage, more hubs can be designed to enhance the scale-free and small-world properties of the CINet, which can provide more paths and shorten the path distances for travelers. This is especially important for those hub vertices that connect multiple transportation modes and have a high number of connections, such as Nanjing South Railway Station, Suzhou Railway Station, and Lukou Airport in this study. Moreover, the selection and design of operation hub vertices in the planning stage are crucial for network robustness. Optimized design of operation hub vertices can effectively strengthen the density of the layout of operational lines, particularly the connectivity between various operation vertices within the same city. This significantly contributes to network robustness enhancement.

2) In the construction stage, whether in the CINet or CONet, a hub with powerful transfer facilities is recommended. The construction of internal transfer channels and external sections of the hubs can not only provide physical separation among different directions and different transportation modes, but also greatly improve network robustness. This design can ensure transportation operation under emergency scenarios and minimize the system loss. For example, when a pandemic occurs, it is necessary to block the transportation of certain directions at the hub to prevent the spread of an epidemic. In this case, only a portion of the passengers from certain channels will be restricted, without affecting the normal transportation operations of other channels.

3) In the management stage, considering that the role of the hub is more important in the CONet

than in the CINet, it is necessary to ensure that the hubs of the same scale operate an equivalent number of lines. It can considerably reduce the negative impact on the robustness of the CONet when high-degree hub vertex failures occur. Furthermore, if network optimization is required in the future and the optimization costs are limited, it is suggested to focus on optimizing the hub vertices in the CONet rather than the CINet. Such measures can lead to more efficient improvements in network robustness.

However, this article also has certain limitations. We only analyze the static robustness of the network and have not considered the dynamic impacts of travel demand variations or the capacity of vertices and edges on network robustness. Further research could employ weighted network analysis to address these aspects. Moreover, the proposed methods in this article should be extended to other regional multimodal comprehensive transportation networks, such as the Beijing-Tianjin-Hebei Urban Agglomeration and Guangdong–Hong Kong–Macao Greater Bay Area, for robustness analysis and validation.

Use of AI tools declaration

The authors declare they have not used Artificial Intelligence (AI) tools in the creation of this article.

Acknowledgments

This research is supported by the National Natural Science Foundation of China (52432010), the National Key Research and Development Program of China (2022XAGG0126), the Zhishan Scholars Programs of Southeast University (2242021R40021), and the China Scholarship Council Program (202406090279).

Conflict of interest

The authors declare there is no conflict of interest.

References

1. L. F. Xiong, *Analysis of Cascading Failure Propagation Mechanism in Comprehensive Transportation Infrastructure Network*, Ph.D thesis, Southwest Jiaotong University, 2019.
2. J. Y. Guo, *Approach to Passenger Flow Regulation of Urban Mass Transit Network*, Ph.D. thesis, Beijing Jiaotong University, 2016.
3. V. Nicolosi, M. Augeri, M. D'Apuzzo, A. Evangelisti, D. Santilli, A probabilistic approach to the evaluation of seismic resilience in road asset management, *Int. J. Dis. Risk Sci.*, **13** (2022),114–124. https://doi.org/ 10.1007/s13753-022-00395-5
4. O. Fröidh, Perspectives for a future high-speed train in the Swedish domestic travel market. *J. Transp. Geogr.*, **4** (2008), 16:268–277. https://doi.org/10.1016/j.jtrangeo.2007.09.005
5. P. Sen, S. Dasgupta, A. Chatterjee, P. A. Sreeram, G. Mukherjee, S. S. Manna, Small-world properties of the Indian railway network. *Phys. Rev. E*, **67** (2003). http://dx.doi.org/10.1103/PhysRevE.67.036106
6. C. von Ferber, T. Holovatch, Y. Holovatch, V. Palchykov, Network harness: Metropolis public transport, *Phys. A*, **380** (2007), 585–591. https://doi.org/ 10.1016/J.PHYSA.2007.02.101

7. Z. X. Wu, H. K. W. Lam, Network equilibrium model for congested multi-mode transport network with elastic demand, *J. Adv. Transp.*, **37** (2003), 295–318. https://doi.org/10.1002/atr.5670370304
8. C. Cao, Y. Su, Transportation infrastructure and regional resource allocation, *Cities*, **155** (2024), 105433. https://doi.org/10.1016/j.cities.2024.105433
9. R. Liu, *Measurement of Economic Growth Effect of High-speed Transportation Network in Urban Agglomerations—Taking the Pearl River Delta as an example*, Ph.D thesis, Yunnan University of Finance and Economics, 2021.
10. N. Zhang, A. Alipour, Multi-scale robustness model for highway networks under flood events, *Transp. Res. D-Tr. E.*, **83** (2020), 102281. https://doi.org/10.1016/j.trd.2020.102281
11. W. H. Zhu, S. D. Wang, S. L. Liu, X. Y. Gao, P. C. Zhang, L. X. Zhang, Reliability and robustness assessment of highway networks under multi-hazard scenarios: a case study in Xinjiang, China, China, *Sustainability*, **15** (2023), 5379. https://doi.org/10.3390/su15065379
12. G. Vani, H. Maoh, Characterizing the nature of a multi-regional trucking network using the network robustness index: An application to Ontario, Canada, *Appl. Spat. Anal. Policy*, **16** (2023), 383–407. https://doi.org/10.1007/s12061-022-09484-w
13. M. Ouyang, C. Liu, M. Xu, Value of resilience-based solutions on critical infrastructure protection: Comparing with robustness-based solutions, *Reliab. Eng. Syst. Saf.*, **190** (2019), 106506. https://doi.org/10.1016/j.ress.2019.106506
14. Y. H. Yang, Y. X. Liu, M. X. Zhou, F. X. Li, C. Sun, Robustness assessment of urban rail transit based on complex network theory: A case study of the Beijing Subway, *Saf. Sci.*, **79** (2015), 149–162. https://doi.org/10.1016/j.ssci.2015.06.006
15. F. Ma, W. J. Shi, K. F. Yuen, Q. P. Sun, X. B. Xu, Y. J. Wang, et al., Exploring the robustness of public transportation for sustainable cities: A double-layered network perspective, *J. Clean. Prod.*, **265** (2020), 121747. https://doi.org/10.1016/j.jclepro.2020.121747
16. S. Wandelt, Y. F. Xu, X. Q. Sun, Measuring node importance in air transportation systems: On the quality of complex network estimations, *Reliab. Eng. Syst. Saf.*, **240** (2023), 109596. https://doi.org/10.1016/j.ress.2023.109596
17. V. Latora, M. Marchiori, Is Boston subway a small-world network?, *Phys. A*, **314** (2002), 109–113. https://doi.org/10.1016/S0378-4371(02)01089-0
18. J. Sienkiewicz, J. A. Hołyst, Statistical analysis of 22 public transport networks in Poland, *Phys. Rev. E*, **72** (2005), 046127. https://doi.org/10.1103/PhysRevE.72.046127
19. G. Domenico, M. Ernesto, Compared analysis of metro networks supported by graph theory, *Networks Spat. Econ.*, **5** (2005), 395–414. https://doi.org/10.1007/s11067-005-6210-5
20. Y. Wang, O. Zhao, L. M. Zhang, Modeling urban rail transit system resilience under natural disasters: A two-layer network framework based on link flow, *Reliab. Eng. Syst. Saf.*, **241** (2024). https://doi.org/10.1016/j.ress.2023.109619
21. M. T. Trobajo, M. V. Carriegos, Spanish airport network structure: Topological characterization, *Comput. Math. Methods*, **2022** (2022), 4952613. https://doi.org/10.1155/2022/4952613
22. M. Zanin, S. Wandelt, An overview of network structures and node importance in the global aviation system from the year 2011 to 2022, *J. Air. Transp. Res. Soc.*, **1** (2023), 63–80. https://doi.org/10.59521/5E2DDEC9FAD4593B
23. K. Sugishita, K. Arisawa, S. Hanaoka, Delay propagation patterns in Japan's domestic air transport network, *Transp. Res. Interdiscip. Perspect.*, **27** (2024), 101235. https://doi.org/10.1016/j.trip.2024.101235

24. N. Anna, D. June, *Supernetworks: Decision-Making for the Information Age*, England: Edward Publishing, Incorporated, 2002.
25. S. C. Dafermos, The traffic assignment problem for multiclass-user transportation networks, *Transp. Sci.*, **6** (1972), 73–87. https://doi.org/10.1287/trsc.6.1.73
26. M. Beuthe, B. Jourquin, J. F. Geerts, C. K. à Ndjang'Ha, Freight transportation demand elasticities: a geographic multimodal transportation network analysis, *Transp. Res. Part E: Logist. Transp. Rev.*, **37** (2001), 253–266. https://doi.org/10.1016/S1366-5545(00)00022-3
27. P. Xu. Intercity multi-modal traffic assignment model and algorithm for urban agglomeration considering the whole travel process, in *IOP Conference Series: Earth and Environmental Science*, **189** (2018), 6. https://doi.org/10.1088/1755-1315/189/6/062016
28. H. Y. Ding, *Research on Urban Multi-Modal Public Transit Network Fast Construction Method and Assignment Model*, Ph.D thesis, Southeast University, 2018.
29. Y. Luo, D. L. Qian, Construction of subway and bus transport networks and analysis of the network topology characteristics, *J. Transp. Syst. Eng. Inf. Technol.*, **15** (2015), 39–44. https://doi.org/10.16097/j.cnki.1009-6744.2015.05.006
30. X. H. Li, J. Y. Guo, C. Gao, Network-based transportation system analysis: A case study in a mountain city, *Chaos, Solitons Fractals*, **107** (2018), 256–265. https://doi.org/10.1016/j.chaos.2018.01.010
31. X. Feng, S. W. He, G. Y. Li, J. S. Chi, Transfer network of high-speed rail and aviation: Structure and critical components, *Phys. A*, **581** (2021), 126197. https://doi.org/10.1016/j.physa.2021.126197
32. X. Q. Huang, J. X. Gao, S. V. Buldyrev, S. Havlin, H. E. Stanley, Robustness of interdependent networks under targeted attack, *Phys. Rev. E*, **83** (2011), 065101. https://doi.org/10.1103/PhysRevE.83.065101
33. B. Berche, C. V. Ferber, T. Holovatch, Y. Holovatch, Resilience of public transport networks against attacks, *Eur. Phys. J. B*, **71** (2009), 125–137. https://doi.org/10.1140/epjb/e2009-00291-3
34. Y. S. Chen, X. Y. Wang, X. W. Song, J. L. Jia, Y. Y. Chen, W. L. Shang, Resilience assessment of multimodal urban transport networks, J. *Circuits Syst. Comput.*, **31** (2022), 18. https://doi.org/10.1142/S0218126622503108
35. L. Ge, S. Voß, L. Xie, Robustness and disturbances in public transport, *Publ. Transp.*, **14** (2022), 191–261. https://doi.org/10.1007/s12469-022-00301-8
36. X. L. Hu, J. Huang, F. Shi, A robustness assessment with passenger flow data of high-speed rail network in China, *Chaos, Solitons Fractals*, **165** (2022), 112792. https://doi.org/10.1016/j.chaos.2022.112792
37. R. S. Yang, W. Sun, M. L. Le, H. Y. Zhang, The Chinese aviation network: An empirical temporal analysis on its structural properties and robustness, *Appl. Sci.*, **13** (2023), 11627. https://doi.org/10.3390/app132111627
38. X. Qu, H. Lin, Y. Liu, Envisioning the future of transportation: Inspiration of ChatGPT and large models, *Commun. Transp. Res.*, **3** (2023), 100103. https://doi.org/10.1016/j.commtr.2023.100103
39. Y. Fei, P. Shi, Y. Liu, L. Wang, Critical roles of control engineering in the development of intelligent and connected vehicles, *J. Int. Connected Veh.*, **7** (2024), 79–85. https://doi.org/10.26599/JICV.2023.9210040

40. S. Y. Kuang, Y. Liu, X. Wang, X. H. Wu, Y. T. Wei, Harnessing multimodal large language models for traffic knowledge graph generation and decision-making, *Commun. Transp. Res.*, **4** (2024), 100146. https://doi.org/10.1016/j.commtr.2024.100146
41. Y. Liu, F. Y. Wu, Z. Y. Liu, K. Wang, F. Y. Wang, X. B. Qu, Can language models be used for real-world urban-delivery route optimization, *The Innovation*, **4** (2023), 6. https://doi.org/10.1016/j.xinn.2023.100520
42. Z. C. Chen, C. J. Zheng, T. T. Tao, Y. Y. Wang, Reliability analysis of urban road traffic network under targeted attack strategies considering traffic congestion diffusion, *Reliab. Eng. Syst. Saf.*, **248** (2024), 110171. https://doi.org/10.1016/j.ress.2024.110171
43. Z. L. Ma, D. W. Hu, S. I. J. Chien, J. Liu, Y. Liu, K. Wu, Robustness of urban rail transit networks considering cascade failure under attacks: A case study of Nanjing, China, *ASCE-ASME J. Risk U. A*, **11** (2025), 04024093. https://doi.org/10.1061/AJRUA6.RUENG-1324
44. T. Li, L. L. Rong, K. S. Yan, Vulnerability analysis and critical area identification of public transport system: A case of high-speed rail and air transport coupling system in China, *Transp. Res. Part A Policy Pract.*, **127** (2019), 55–70. https://doi.org/10.1016/j.tra.2019.07.008
45. Y. Chen, J. E. Wang, F. J. Jin, Robustness of China's air transport network from 1975 to 2017, *Phys. A*, **539** (2020), 122876. https://doi.org/10.1016/j.physa.2019.122876
46. S. Wandelt, X. Shi, X. Q. Sun, Estimation and improvement of transportation network robustness by exploiting communities, *Reliab. Eng. Syst. Saf.*, **206** (2021), 107307. https://doi.org/10.1016/j.ress.2020.107307
47. Z. Xin, F. Niu, Structure and robustness of China's railway transport network, *Transp. Lett.*, **15** (2023), 375–385. https://doi.org/10.1080/19427867.2022.2053280
48. V. H. Tran, S. A. Cheong, N. D. Bui, Complex network analysis of the robustness of the hanoi, vietnam bus network, *J. Syst. Sci. Complex*, **32** (2019), 1251–1263. https://doi.org/10.1007/s11424-019-7431-x
49. Y. T. Zheng, J. L. Xiao, X. D. Hua, W. Wang, H. Chen, A comparative analysis of the robustness of multimodal comprehensive transportation network considering mode transfer: A case study, *Electron. Res. Arch.*, **31** (2023), 5362–5395. https://doi.org/10.3934/era.2023272
50. T. Li, L. L. Rong, A comprehensive method for the robustness assessment of high-speed rail network with operation data: A case in China, *Transp. Res. Part A Policy Pract.*, **132** (2020), 666–681. https://doi.org/10.1016/j.tra.2019.12.019
51. Y. Zhou, J. Wang, G. Q. Huang, Efficiency and robustness of weighted air transport networks, *Transp. Res. Part E: Logist. Transp. Rev.*, **122** (2019), 14–26. https://doi.org/10.1016/j.tre.2018.11.008
52. J. C. Jiang, L. X. Wu, J. Q. Yu, M. J. S. Wang, K. Hui, Z.X. Zhang, et al., Robustness of bilayer railway-aviation transportation network considering discrete cross-layer traffic flow assignment, *Transp. Res. D-Tr. E*, **127** (2024), 104071. https://doi.org/10.1016/j.trd.2024.104071
53. J. H. Zhang, Y. Zhou, S. L. Wang, Q. J. Min, Critical station identification and robustness analysis of urban rail transit networks based on comprehensive vote-rank algorithm, *Chaos, Solitons Fractals*, **178** (2024), 114379. https://doi.org/10.1016/j.chaos.2023.114379
54. Y. F. Zhang, S. T. Ng, Robustness of urban railway networks against the cascading failures induced by the fluctuation of passenger flow, *Reliab. Eng. Syst. Saf.*, **219** (2022), 108227. https://doi.org/10.1016/j.ress.2021.108227

55. Z. Z. Liu, H. Chen, E. Z. Liu, W. Y. Hu, Exploring the resilience assessment framework of urban road network for sustainable cities, *Phys. A*, **586** (2022), 126465. https://doi.org/10.1016/j.physa.2021.126465